

 Open access • Posted Content • DOI:10.1101/033787

Across-cohort QC analyses of genome-wide association study summary statistics from complex traits — Source link

Guo-Bo Chen, Sang Hong Lee, Matthew R. Robinson, Maciej Trzaskowski ...+13 more authors

Institutions: University of Queensland, University of North Carolina at Chapel Hill, University of Exeter, University of Michigan ...+3 more institutions

Published on: 06 Dec 2015 - bioRxiv (bioRxiv)

Topics: Statistic and Genome-wide association study

Related papers:

- [Across-cohort QC analyses of GWAS summary statistics from complex traits](#)
- [Dealing with heterogeneity between cohorts in genomewide SNP association studies.](#)
- [metaCCA: Summary statistics-based multivariate meta-analysis of genome-wide association studies using canonical correlation analysis](#)
- [Proper conditional analysis in the presence of missing data: Application to large scale meta-analysis of tobacco use phenotypes](#)
- [Evaluation and application of summary statistic imputation to discover new height-associated loci](#)

Share this paper:    

View more about this paper here: <https://typeset.io/papers/across-cohort-qc-analyses-of-genome-wide-association-study-1jebyztuvq>

1 **Title:** Across-cohort QC analyses of genome-wide association study summary statistics from complex traits

2

3 **Authors:** Guo-Bo Chen¹, Sang Hong Lee^{1,2}, Matthew R Robinson¹, Maciej Trzaskowski¹, Zhi-Xiang Zhu³,
4 Thomas W Winkler⁴, Felix R Day⁵, Damien C Croteau-Chonka^{6,7}, Andrew R Wood⁸, Adam E Locke⁹,
5 Zoltán Kutalik¹⁰⁻¹², Ruth J F Loos¹³⁻¹⁵, Timothy M Frayling⁸, Joel N Hirschhorn¹⁶⁻¹⁹, Jian Yang^{1,21}, Naomi R
6 Wray¹, The Genetic Investigation of Anthropometric Traits (GIANT) Consortium²⁰, Peter M Visscher^{1,21}

7

8 **Affiliations:**

9 ¹ Queensland Brain Institute, The University of Queensland, Brisbane, Queensland, Australia

10 ² School of Environmental and Rural Science, The University of New England, Armidale, New South
11 Walsh, Australia

12 ³ SPLUS Game, Guangzhou, Guangdong, China

13 ⁴ Department of Genetic Epidemiology, Institute of Epidemiology and Preventive Medicine, University of
14 Regensburg, Regensburg, Germany

15 ⁵ Medical Research Council (MRC) Epidemiology Unit, Institute of Metabolic Science, Addenbrooke's
16 Hospital, Cambridge, UK

17 ⁶ Department of Genetics, University of North Carolina, Chapel Hill, North Carolina, USA

18 ⁷ Channing Division of Network Medicine, Department of Medicine, Brigham and Women's Hospital and
19 Harvard Medical School, Boston, Massachusetts, USA

20 ⁸ Genetics of Complex Traits, University of Exeter Medical School, University of Exeter, Exeter, UK

21 ⁹ Department of Biostatistics and Center for Statistical Genetics, University of Michigan, Ann Arbor,
22 Michigan, USA

23 ¹⁰ Department of Medical Genetics, University of Lausanne, Lausanne, Switzerland

24 ¹¹ Institute of Social and Preventive Medicine (IUMSP), Centre Hospitalier Universitaire Vaudois (CHUV),
25 Lausanne, Switzerland

26 ¹² Swiss Institute of Bioinformatics, Lausanne, Switzerland

27 ¹³ The Charles Bronfman Institute for Personalized Medicine, Icahn School of Medicine at Mount Sinai,
28 New York, New York, USA

29 ¹⁴ The Mindich Child Health and Development Institute, Icahn School of Medicine at Mount Sinai, New
30 York, New York, USA

31 ¹⁵ The Genetics of Obesity and Related Metabolic Traits Program, Icahn School of Medicine at Mount Sinai,
32 New York, New York, USA

33 ¹⁶ Department of Genetics, Harvard Medical School, Boston, Massachusetts, USA

34 ¹⁷ Program in Medical and Population Genetics, Broad Institute of MIT and Harvard, Cambridge,
35 Massachusetts, USA

36 ¹⁸ Center for Basic and Translational Obesity Research, Boston Children's Hospital, Boston, Massachusetts,
37 USA

38 ¹⁹ Division of Endocrinology, Boston Children's Hospital, Boston, Massachusetts, USA

39 ²⁰ A full list of members is available in the **Supplementary Note**

40 ²¹ The University of Queensland Diamantina Institute, Translation Research Institute, Brisbane, Queensland,
41 Australia

42

43 **Correspondence should be addressed to**

44 GBC (chen.guobo@foxmail.com) or PMV (peter.visscher@uq.edu.au)

45 **Running title:** Four metrics for GWAMA

46 **Keywords:** meta-analysis, overlapping samples, meta-PCA, Fst, PPSR, GIANT, MetaboChip

47

48

Abstract

49 Genome-wide association studies (GWASs) have been successful in discovering replicable SNP-trait
50 associations for many quantitative traits and common diseases in humans. Typically the effect sizes of SNP
51 alleles are very small and this has led to large genome-wide association meta-analyses (GWAMA) to
52 maximize statistical power. A trend towards ever-larger GWAMA is likely to continue, yet dealing with
53 summary statistics from hundreds of cohorts increases logistical and quality control problems, including
54 unknown sample overlap, and these can lead to both false positive and false negative findings. In this study
55 we propose a new set of metrics and visualization tools for GWAMA, using summary statistics from cohort-
56 level GWASs. We proposed a pair of methods in examining the concordance between demographic
57 information and summary statistics. In method I, we use the population genetics F_{st} statistic to verify the
58 genetic origin of each cohort and their geographic location, and demonstrate using GWAMA data from the
59 GIANT Consortium that geographic locations of cohorts can be recovered and outlier cohorts can be
60 detected. In method II, we conduct principal component analysis based on reported allele frequencies, and is
61 able to recover the ancestral information for each cohort. In addition, we propose a new statistic that uses the
62 reported allelic effect sizes and their standard errors to identify significant sample overlap or heterogeneity
63 between pairs of cohorts. Finally, to quantify unknown sample overlap across all pairs of cohorts we propose
64 a method that uses randomly generated genetic predictors that does not require the sharing of individual-
65 level genotype data and does not breach individual privacy.

66

67

Introduction

68 Genome-wide association studies (GWASs) have been successful in discovering SNP-trait associations for
69 complex traits¹. To elucidate genetic architecture, which requires maximized statistical power for discovery
70 of risk alleles of small effect, large genome-wide association meta-analyses (GWAMA) are tending towards
71 ever-larger scale that may contain data from hundreds of cohorts. At the individual cohort level, GWAS
72 analysis is often based on various genotyping chips and conducted with different protocols, such as different
73 software tools and reference populations for imputation, inclusion of study specific covariates and
74 association analyses using different methods and software. Although solid quality control analysis pipelines
75 of GWAMA exist², these analyses focus on quality control (QC) for each cohort independently. With ever-
76 increasing sizes of GWAMA there is a need for additional QC that goes beyond the cohort-by-cohort
77 genotype-level analysis performed to date.

78

79 In this study, we propose a new set of QC metrics for GWAMA. In contrast to previous QC metrics, our
80 approach explores the genetic and QC context of the all cohorts in GWAMA together rather than by treating
81 them one at a time. These metrics include

82 (i) a genome-wide comparison of allele frequency differences across cohorts or against a common reference
83 population

84 (ii) principal component analysis for reported allele frequencies

85 (iii) a pairwise cohort statistic that uses allele frequency or effect size concordance to detect the proportion
86 of sample overlap or heterogeneity

87 (vi) an easy to implement analysis to pinpoint each between-cohort overlapping sample that does not require
88 the sharing of individual-level genotype data.

89

90 All these applications assume that there is a central analysis hub where summary statistic data from GWAS
91 are uploaded for each cohort. In addition, these metrics reveal information of interest other than merely QC.

92

93

Materials and Methods

94 Overview of materials

95 **Cohort-level summary statistics.** The GWAS height GWAS summary statistics were provided by the
96 GIANT Consortium and were from 82 cohorts (174 separate files due to different ways a cohort was split
97 into different sexes, different disease statuses) representing a total of 253,288 individuals, and nearly 2.5
98 million autosome SNPs imputed to the HapMap2 reference³. The MetaboChip summary statistics were for
99 body mass index (BMI) from 43 cohorts (120 files due to different ways a cohort was split into different
.00 sexes, different disease statuses) representing a total of 103,047 samples from multiple ethnicities with about
.01 200,000 SNPs genotyped on customised chips^{4,5}. For convenience, we consider each file a cohort. All the
.02 summary statistics have already been cleaned using established protocols for GWAS meta-analysis².

.03
.04 **1000 Genomes Project samples.** 1000 Genomes Project (1KG) reference samples⁶ were used as the
.05 reference samples for calculating F_{st} . When assessing the global-level F_{st} measures, Yoruba represent
.06 African samples (YRI, 108 individuals), Han Chinese in Beijing represent East Asian samples (CHB, 103
.07 individuals), and Utah Residents with Northern and Western European Ancestry represent European samples
.08 (CEU, 99 individuals) were employed as the reference panels. For calculating within-Europe F_{st} , CEU,
.09 Finnish (FIN, 99 individuals), and Tuscani (TSI, 107 individuals) were employed to represent northwest,
.10 northeast and southern Europeans, respectively. For analyses using a whole European panel, CEU, FIN, TSI,
.11 GBR (British, 91 individuals), and IBS (Iberian, 107 individuals) were pooled together as an “averaged”
.12 European reference.

.13
.14 **WTCCC GWAS data.** WTCCC GWAS data has 2,934 shared controls for 7 diseases with a total of 14,000
.15 cases⁷. Individual GWAS was conducted for each disease using PLINK⁸, and their summary statistics used
.16 to estimate λ_{meta} (see text below). WTCCC GWAS data were also used for demonstrating pseudo profile
.17 score regression (see text below).

.18
.19 **Simulated cohort-level summary statistics.** M independent loci were generated for cohort-level summary
.20 statistics. Each locus had allele frequency p_i , which was sampled from a uniform distribution ranging from
.21 0.1 to 0.5, and had genetic effect b_i , sampled from a standard normal distribution $N(0,1)$. After rescaling,
.22 $\sum_{i=1}^M 2p_i(1-p_i)b_i^2 = h^2$. p and b were treated as true parameters. For a particular cohort with n samples, its
.23 $\tilde{p}_i \sim N(p_i, \frac{p_i(1-p_i)}{2n})$, $\tilde{b}_i \sim N(b_i, \frac{1}{2np_i(1-p_i)})$, and the sampling variance for \tilde{b}_i is $\sigma_{\tilde{b}_i}^2 = \frac{1}{2np_i(1-p_i)}$. All cohorts
.24 were assumed to share common genetic architecture, and differences were only due to genetic drift, allele
.25 frequencies and sampling variance of genetic effects.

.26

.27 **Overview of the methods**

.28 **F_{st} -based genetic distance between cohorts.** For a cohort, its F_{st} with reference cohorts, such as CEU, YRI,
.29 and CHB, is calculated. Given those three F_{st} values, the coordinate of this cohort can be uniquely projected
.30 into the reference equilateral that has CEU, YRI, and CHB at its corners.

.31

.32 **Principal component analysis for cohort-level allele frequencies.** A genetic relationship matrix for
.33 cohorts can be constructed based on received allele frequencies. Principal component analysis (PCA) can be
.34 implemented on the genetic relationship matrix. The projection of the cohorts into PCA space can reveal the
.35 genetic background and relative geographical distance between cohorts.

.36

.37 **λ_{meta} for detecting overlapping samples.** In concept, λ_{meta} resembles λ_{gc} , which indicates population
.38 stratification for a GWAS⁹, but λ_{meta} measures the proportion of overlapping samples between a pair of

.39 cohorts. Based on reported genetic effects and their sampling variance, λ_{meta} can be constructed for a pair of
.40 cohorts and follows a chi-square distribution with 1 degree of freedom. λ_{meta} will be close to 1 when there
.41 is no overlapping samples, smaller than 1 when there are overlapping samples, and greater than 1 when there
.42 are heterogeneity between a pair of cohorts. For GWAMA over a single trait across method, we assume
.43 heterogeneity is zero.

.44

.45 **Pseudo profile score regression for pinpointing overlapping samples/relatives.** Pseudo profile score
.46 regression (PPSR) provides a framework for pinpointing the overlapping samples/relatives between cohort
.47 without sharing genotypes. Each GWAS analyst generates pseudo profile scores (PPS) for each sample on a
.48 set of loci, which are chosen by a GWAMA central analyst. If the similarity metric of PPS for a pair of
.49 cohorts reaches a similarity threshold, say 1 overlapping samples and 0.5 for first-degree relatives, then
.50 overlapping samples/relatives are found. PPSR can have a controlled type-I and type-II error rates in
.51 pinpointing overlapping samples, and also can reduce the comprise of privacy. PPSR is an enhanced version
.52 of Gencrypt¹⁰, a previous method in pinpointing overlapping samples.

.53

.54 The technical details of these four methods can be found in the Supplementary notes.

.55

.56

Results

.57 **Population genetic quality control analysis using F_{st}**

.58 Allele frequency differentiation among populations reflects population characteristics such as demographic
.59 past and geographic locations^{11,12}. In GWAMA only summary statistics such as allele frequencies are
.60 available to the central analysis hub, and so it is not possible to run principal component analysis for each
.61 cohort that requires individual-level data. Therefore it is difficult to quantify genetic distance between
.62 cohorts or to a reference in order to identify population outliers. Outlier cohorts can be due to real
.63 differences in ethnicity or mistakes in the primary analysis prior to uploading data to the GWAMA analysis
.64 hub. Gross differentiation in allele frequencies at specific SNPs between GWAMA cohorts and a reference
.65 (such as 1000 Genomes Project, denoted as 1KG)⁶ are part of standard QC protocols² but checking for more
.66 differentiation than expected across the entire genome is not usually part of the QC pipeline. We propose
.67 that a genetic distance inferred from F_{st} , which reflects genetic distance between pairwise populations, is a
.68 useful additional QC statistic to detect cohorts that are population outliers. Using the relationship between
.69 F_{st} and principal components¹³⁻¹⁵, our F_{st} Cartographer algorithm can be used to estimate the relative
.70 genetic distance between cohorts (**Supplementary notes, and Supplementary Fig. 1**).

.71

.72 We applied the F_{st} metric to the GIANT Consortium body mass index (BMI) MetaboChip cohorts (55 male-
.73 only cohorts, 55 female-only cohort, and 10 mixed-sex cohorts; for convenience, we called each file a
.74 cohort), which were recruited from multiple ethnicities⁴, such as Europeans, African Americans in The

.75 Atherosclerosis Risk in Communities Study (ARIC) and cohorts from Jamaica (SPT), Pakistan (PROMISE),
.76 Philippines (CLHNS) and Seychelles (SEY). For each MetaboChip cohort, we sampled 30,000 (see Online
.77 method for details) independent markers to calculate F_{st} values with each of three 1KG samples (CEU, CHB,
.78 and YRI, respectively). For validation of the method, we also calculated F_{st} values against the 1KG
.79 Japanese (JPT, Japanese in Tokyo, Japan), Indian (GIH, Gujarati Indian in Houston, US), Kenyan (LWK,
.80 Luhya in Webuye, Kenya) and European samples (IBS, Iberian populations, Spain; FIN, Finnish, Finland;
.81 TSI, Toscani, Italy, and GBR, British in England and Scotland, GBR), to see whether the known genetic
.82 origins of those cohorts can be recovered.

.83

.84 According to the origins of the samples, each MetaboChip cohort showed a different genetic distance
.85 spectrum to the three reference populations (**Fig. 1a**). The JPT and Philippine cohorts had very small genetic
.86 distances to CHB, as expected, but large to CEU and YRI; however, the Pakistan cohorts showed much
.87 closer genetic distances to CEU than to CHB and YRI, indicating their demographic history. The cohorts
.88 sampled from Jamaica, Seychelles, Hawaii, and the African American ARIC cohort had small genetic
.89 distances to YRI, but large distances to CHB and CEU. For most European cohorts, as expected, the
.90 distances to CEU were very small compared with those to CHB and YRI. Given their relative distances to
.91 CEU, CHB, and YRI, using our F_{st} cartographer algorithm (**Supplementary notes, and Supplementary**
.92 **Fig. 1**), the cohorts were projected into a two-dimensional space, called F_{st} derived principal components
.93 (F_{PC}) space, constructed by YRI, CHB, and CEU as the reference populations (**Fig. 1b**). The allocation of
.94 the cohorts to the F_{PC} space resembles that of eigenvector 1 against eigenvector 2 in principal component
.95 analysis (PCA)¹², and is similar to those observed in PCA using individual-level GWAS data for populations
.96 of various ethnicities such as in 1KG samples⁶. Therefore, our method to place cohorts in geographical
.97 regions from GWAS summary statistics works well at a global-population scale.

.98

.99 We next investigated whether our genetic distance method works at a much finer geographic scale. It is
:00 known that using individual-level data, principal component analysis can mirror the geographic locations for
:01 European samples¹¹. Here, we analyzed the 103 GIANT European-ancestry MetaboChip cohorts (48 male-
:02 only cohorts, 47 female-only cohorts, and 8 mix-sex cohorts) for fine-scale F_{st} genetic distance measure by
:03 using the CEU, FIN, and TSI reference populations, which represent northwest, northeast, and southern
:04 European populations, respectively. For each of the GIANT European-ancestry MetaboChip cohorts, F_{st} was
:05 calculated relative to each of these three reference populations and showed concordance with the known
:06 origin of the samples (**Fig. 1c**). For example, cohorts from Finland and Estonia were close to FIN but distant
:07 to TSI; cohorts from South Europe such as Italy and Greece had small genetic distance to TSI; and cohorts
:08 from West European nations had small genetic distance to CEU. Similarly, the projected origin for each
:09 European-ancestry MetaboChip cohort resembles their geographic location within the European map as

!10 expected (**Fig. 1d**). Therefore, our QC measure based upon population differentiation also works at a fine
!11 scale.

!12

!13 We next applied the F_{st} genetic distance measures to 174 GIANT height GWAS cohorts (79 male-only
!14 cohorts, 76 female-only cohorts, and 19 mixed-sex cohorts; excluding MetaboChip data), which were all of
!15 European ancestry imputed to the HapMap reference panel³. Given the three F_{st} values to CEU, FIN, and
!16 TSI (**Fig. 2a**), the geographic origin for each cohort can be inferred as for the GIANT BMI MetaboChip data
!17 (**Supplementary notes**). The projected coordinates of each GWAS cohort matches its origin very well (**Fig.**
!18 **2b**). For example, a Canadian cohort, the Quebec Family Study (QFS), was closely located to DESIR, a
!19 French cohort, consistent with the French genetic heritage of the QFS¹⁶. In addition, we also observe
!20 complexity due to mixed samples from different countries. For example, the DGI/Botnia study had samples
!21 recruited from Sweden and Finland, and its inferred geographic location is in between of the Swedish
!22 cohorts and Finnish cohorts¹⁷. We also note that for the MIGN consortium cohorts, which are from Finland,
!23 Sweden, Spain and the US, the same allele frequencies were reported for all their sub-cohorts, and all
!24 cohorts were allocated to southern Europe (very closely located to 1KG IBS cohort; **Fig. 2b and**
!25 **Supplementary Fig. 2**). As the allele frequencies, used in QC steps to eliminate low quality loci, were not
!26 directly used in estimating genetic effects in the GWAMA, the reported allele frequencies in MIGN have
!27 not impacted on the published GWAMA results³.

!28

!29 Next, we show that F_{st} can detect populations that have a different demographic past. Using all 1KG
!30 European samples as the reference panel (that is, an “averaged” European reference panel), most cohorts in
!31 GIANT had $F_{st} < 0.005$ with this average, which agrees with previously reported results using individual
!32 level data from European nations¹¹. A few cohorts showed large F_{st} , such as the AMISH cohort with
!33 $F_{st} = 0.018$, and the North Swedish Population Health Study (NSPHS)¹⁸ with $F_{st} = 0.014$. Consistent with
!34 these results, both these populations are known to have been genetically isolated (**Supplementary Fig. 3**).

!35

!36 **Principal component analysis for allele frequencies**

!37 It is well established that given individual-level data principal component analysis (PCA) can reveal the
!38 ancestral information for samples¹². Given the same allele frequencies as used for F_{st} -based analysis above,
!39 we conducted PCA for allele frequencies, denoted as meta-PCA. In meta-PCA each cohort was analogously
!40 considered as an “individual”. For example, 120 MetaboChip cohorts were considered as a sample of 120
!41 “individuals”. Although the inferred ancestral information was for each cohort rather than any individuals,
!42 implementation of meta-PCA was the same as the conventional PCA (**Supplementary Notes**).

!43

!44 Meta-PCA was tested with 1KG samples over nearly 1 million SNPs. The cohort-level allele frequencies
!45 were calculated first for 26 1KG cohorts, and meta-PCA was conducted. The projected cohorts were

!46 consistent to their genetic origin (**Fig. 3**). In contrast, conventional PCA was also conducted on 1KG
!47 individual genotypes directly, and the mean coordinates for each cohort was then calculated. As illustrated in
!48 Fig. 3, these two techniques resulted in nearly identical projection for 1KG, and the correlation between
!49 cohort coordinates remained consistently high for the first eight eigenvectors, $R^2 > 0.8$. It indicated that
!50 meta-PCA could reveal genetic background for each cohort as precise as that based on individual-level data.

!51

!52 We applied meta-PCA to 120 MetaboChip cohorts for nearly 34 thousand common SNPs between
!53 MetaboChip and 1KG variants, with the inclusion of 10 1KG cohorts (East Asian: CHB, JPT; South Asian:
!54 GIH; European: CEU, FIN, GBR, IBS, TSI; African: LWK, YRI) as the reference cohorts. Consistent with
!55 demographic information, the inferred ancestral information of each cohort agreed well with demographic
!56 information. For example, PROMISE (Pakistan) located very close to GIH, CLHNS (Philippines) close to
!57 CHB and JPT, ARIC (African American) and SPT (Jamaican) close to YRI and LWK, and the European
!58 cohorts close to CEU and FIN (**Fig 4**).

!59

!60 We also applied meta-PCA to 174 GIANT height GWAS cohorts for nearly 1M SNPs, with the inclusion of
!61 10 1KG reference cohorts. At the global-population level, the 174 cohorts were all allocated close to CEU
!62 and FIN, consistent with their reported demographic information (**Fig. 5**). For fine-scale inference, we
!63 conducted meta-PCA again but with the inclusion of the five European samples. As demonstrated, the
!64 resolution of the inferred relative location between European cohorts reflected their real geographical
!65 locations, as previously observed using individual-level data¹¹.

!66

!67 These results were consistent to what observed from F_{pc} as described in the last section, and also agreed well
!68 with demographic information. So, based on the reported allele frequencies, the demographic information
!69 could be examined by meta-PCA method.

!70

!71 λ_{meta} to detect pairwise cohort heterogeneity and sample overlap

!72 For a single cohort GWAS, λ_{GC} provides a tool for assessing average trait-SNP associations in GWAS⁹, and
!73 an value departing from 1 may indicate undesired phenomena such as population stratification. In this study,
!74 we use the summary statistics for a pair of cohorts to calculate λ_{meta} , a metric that examines heterogeneity
!75 from the concordance of reported effect sizes and sampling variance. We use 30,000 markers in linkage
!76 equilibrium along the genome between a pair of cohorts to estimate λ_{meta} .

!77

!78 For a SNP marker (i), given its reported estimated effect size (b_i) and sampling variance (σ_i^2) in a pair of
!79 cohorts 1 and 2, we can calculate a test statistic $T_i = \frac{(b_{1,i} - b_{2,i})^2}{\sigma_{1,i}^2 + \sigma_{2,i}^2}$, the ratio between the squared difference of
!80 their reported effects to the sum of their reported sampling variances. Under the null hypothesis of no
!81 overlapping samples/heterogeneity, T follows a chi-square distribution with 1 degree of freedom

82 **(Supplementary notes)**. $\lambda_{meta} = \frac{median(T)}{median(\chi_1^2)}$, the ratio between the median of the 30,000 T values and the
83 median of a chi-square statistic with 1 degree of freedom (a value of 0.455), has an expected value of 1 for
84 two independent GWAS summary statistics sets for the same trait. When there is heterogeneity between
85 estimated genetic effects, the expectation is $\lambda_{meta} > 1$, and in contrast $\lambda_{meta} < 1$ if there are overlapping
86 samples. In general, not only overlapping samples but also close relatives present in different cohorts can
87 lead to correlated summary statistics generating $\lambda_{meta} < 1$ **(Supplementary notes)**. However, unless the
88 proportion of overlapping relatives is substantial and their phenotypic correlation is high, the correlation of
89 the summary statistics due to the effective number of overlapping samples (n_o) is expected to be dominated
90 by the same individuals contributing phenotypic and genetic information to different cohorts
91 **(Supplementary Fig. 4)**. Furthermore, if genomic control is applied to adjust the sampling variance¹⁹ then
92 λ_{meta} will be reduced relative to its value without genomic control **(Supplementary notes)**.

93
94 We estimated λ_{meta} from published GWAS summary statistics for a range of traits (other than BMI and
95 height) and were able to find examples of both deflated and inflated λ_{meta} . First, we tested the λ_{meta} on data
96 sets with known overlap. For example, GWAS summary statistics for schizophrenia were available in two
97 phases: the first had 9,394 controls and 12,462 cases²⁰, and in the next phase about 18,000 Swedish samples
98 were added²¹. Such a substantial overlap sample between these two sets of summary statistics led to the
99 estimated value of λ_{meta} as low as 0.257 **(Supplementary Fig. 5)**, consistent with this known overlap. In
100 contrast, heterogeneity between data sets (represented by $\lambda_{meta} > 1$), was observed between GWAS
101 summary statistics of rheumatoid arthritis from European and Asian studies²², for which $\lambda_{meta} = 1.09$
102 **(Supplementary Fig. 6)**. In addition, we note that the distribution of the empirical T -statistics deviates from
103 expectation at the upper tail of the distribution, suggesting differences in effect size or linkage
104 disequilibrium between these two ancestries.

105
106 Next, we estimated λ_{meta} from pairs of cohorts from the 174 GIANT height GWAS cohort³. We found no
107 evidence for substantial sample overlap but do observe between-cohort heterogeneity, and technical artifacts.
108 From the 174 GIANT height GWAS (supplied data files)³, we calculated 15,051 cohort-pairwise λ_{meta}
109 values, resulting in a bell-shape distribution **(Fig. 6a,b)** with the mean of 1.013 and the empirical standard
110 deviation (S.D.) of 0.022, which was greater than theoretical S.D. of 0.014. The empirical mean and S.D can
111 be used to construct a z-score test for each λ_{meta} . These results are consistent with a small amount of
112 heterogeneity, which is not unexpected due to variation of actual (unknown) genetic architecture and
113 analysis protocols. However, the mean is close to 1.0 and based upon this QC metric the results are
114 consistent with stringent quality control and data cleaning. The minimum λ_{meta} value was around 0.88
115 (between SORBS MEN and SORBS WOMEN, **Fig. 3c**), with p -value $< 1e-10$ (testing for the difference
116 from 1), and the maximum was 1.245 (between SARDINIA and WGHS, **Fig. 6d**), with p -value $< 1e-10$,
117 leading to the most deflated and inflated λ_{meta} across GIANT height study cohorts; both were significant

318 after correction for multiple testing. Illustrating λ_{meta} (**Fig. 6b**) highlighted that 20 cohorts from the MIGEN
319 consortium showed substantially lower λ_{meta} with many other cohorts (right-bottom triangle in **Fig. 6b**)
320 than the average, consistent with over-conservative models for statistical association analyses being used in
321 these cohorts – which may be due to very small sample size (ranging from 36 to 320 for the 20 MIGEN
322 cohorts, with an average sample size of 132). Consistent with this, cohorts from MIGEN also have many of
323 their $\lambda_{GC} < 1$ (**Fig. 7a**). In contrast, the SardinIA cohort (4,303 samples) showed heterogeneity with nearly
324 all other cohorts (**Fig. 7b**), perhaps due to unknown artifacts or a slightly different genetic architecture for
325 height as result of demographic history²³.

326

327 We investigated the relationship between $\bar{\lambda}_{meta}$ (the mean of all λ_{meta} values of a given cohort with each of
328 the other 173 GIANT height cohorts) and λ_{GC} among the GIANT height cohorts. If there are no technical
329 issues, such as inflated or deflated sampling variance for the estimated effects, we would expect to see: i) a
330 correlation between λ_{GC} and sample size; ii) no correlation between $\bar{\lambda}_{meta}$ and sample size; iii) no
331 correlation between $\bar{\lambda}_{meta}$ and λ_{GC} (**Supplementary Fig. S7**). Consistent with a previous study²⁴, for a
332 polygenic trait such as height λ_{GC} of each cohort was related to its sample size (correlation of 0.235, $p =$
333 0.0018). In contrast, the correlation between $\bar{\lambda}_{meta}$ and sample size was of 0.116 ($p = 0.127$) (**Fig 7a,b**).
334 Nevertheless, the correlation between the mean of $\bar{\lambda}_{meta}$ and λ_{GC} was 0.836 ($p < 10e-16$) for 174 GIANT
335 height cohorts (**Fig 7c**). We note that the 20 MIGEN cohorts had proportionally small λ_{GC} and $\bar{\lambda}_{meta}$, with
336 very high correlation between them ($\rho = 0.98$); in contrast, the SardinIA cohort, which had the largest λ_{GC} ,
337 showed the largest $\bar{\lambda}_{meta}$ (1.070 ± 0.049), standing out as a special case among the GIANT height cohorts.
338 Assuming a polygenic model of $h^2 = 0.5$ over 30,000 independent loci, we simulated 174 cohorts using the
339 actual size samples from the GIANT height cohorts (**Supplementary notes**), and observed an increased
340 correlation ($R^2 = 0.78$) between $\bar{\lambda}_{meta}$ and λ_{GC} for simulated cohorts with sample sizes of the MIGEN
341 cohorts (**Fig. 7d**). Other effects, such as inflated/deflated sampling variance of the estimated genetic effects
342 could also lead to correlation between $\bar{\lambda}_{meta}$ and λ_{GC} (**Supplementary Fig. S8**). In addition, we constructed
343 a single MIGEN analysis by combining the 20 MIGEN cohorts using an inverse variance weighted meta-
344 analysis²⁵, and calculated λ_{meta} between this combined MIGEN cohort and all 174 cohorts. As expected, the
345 combined MIGEN had $\lambda_{meta} = 0.90 \pm 0.07$ with 20 MIGEN cohorts due to overlapping samples. In
346 contrast, $\lambda_{meta} = 1.01 \pm 0.02$ with 154 other cohorts, was consistent with neither heterogeneity nor sample
347 overlap. Given that the MIGEN (2,340 samples) and SardinIA (4,303 samples) cohorts contributed less than
348 3% of the total sample size (253,288 samples from the GIANT height GWAS cohorts), any impact of
349 unusual λ_{meta} values on the meta-analysis results is very small. Given no heterogeneity between a pair of
350 cohorts, a deflated λ_{meta} reflects the effective number of overlapping samples (**Supplementary notes**). For
351 example, the “combined MIGEN” had λ_{meta} values proportional to the sample size of each MIGEN cohort
352 (**Fig 7e**).

353

354 The statistical power of detection of overlapping samples is maximized when a pair of cohorts has equal
355 sample size (**Fig. 8a**), or in other words the confidence interval for null hypothesis of no overlapping
356 samples depends on the sample sizes for a pair of cohorts. As a comparison, direct correlation that is
357 estimated between the genetic effects for a pair of cohorts has been proposed to estimate overlapping
358 samples^{26,27}, but it is confounded with genetic architecture, such as heritability underlying (**Table 1**). When
359 there was heritability, the estimated correlation between genetic effects was biased and leads to incorrect
360 overlapping samples for a pair of cohorts; when there was no heritability, the estimated correlation was
361 correct and agreed well with the one estimated with λ_{meta} . As existence of heritability is one of the reasons
362 that trigger GWAMA, so λ_{meta} is much proper in estimating overlapping samples between cohorts.

363
364 Another parameterization of λ_{meta} is to estimate it from differences in allele frequencies between a pair of
365 cohorts instead of differences between estimated effect sizes (**Supplementary notes**). We show that λ_{meta}
366 constructed on reported allele frequencies from genotyped loci from summary statistics can detect
367 overlapping samples between two cohorts regardless of whether the GWAS is from quantitative traits or
368 case-control data, even for pairs of different traits (**Supplementary notes and Supplementary notes**). For
369 example, 2,934 common controls were shared across the WTCCC 7 diseases⁷. From the 21 pairwise λ_{meta} ,
370 we estimated a mean of the number of overlapping samples, assuming overlapping controls only
371 (**Supplementary notes**), of $\hat{n}_o = 2,708$ (S.D. = 58.4), which was very close estimate to the actual number of
372 overlapping samples (**Supplementary Fig. 8**). When constructing λ_{meta} on the reported genetic effects and
373 their sampling variance, the estimated mean estimate of the number of shared controls was $\hat{n}_o = 2,127$ (S.D.
374 = 257.7), lower than that estimated from allele frequencies, which is likely due to real genetic heterogeneity
375 between diseases (**Supplementary Fig. 8**). In practice, publically available summary statistics may not
376 include sample specific allele frequencies, but may only be available with reference sample frequencies as a
377 conservative strategy to prevent identification of individuals in a cohort.

378

379 **Detection of overlapping samples using pseudo profile score regression**

380 GWAMAs have grown in sample size and in the number of cohorts that participate, and this trend is likely to
381 continue. The probability that a sample is represented in more than one meta-analysis study is also likely to
382 increase, in particular when very large cohorts such as UK Biobank and 23andMe provide data to multiple
383 studies. While the metric λ_{meta} can be transformed to give an estimate of n_o between cohorts for
384 quantitative traits, it cannot give an estimate of overlapping samples in case-control studies due to the ratio
385 of the cases and controls in each study (**Supplementary notes**). Sharing individual genotype data (or
386 imputed genotypes) across the entire study would make it easy to detect identical or near-identical genotype
387 samples (representing real duplicate samples from individuals who participated in the two studies or
388 monozygotic twins). In fact, only a small number of common SNPs is needed to detect sample overlap, and
389 if this is known then individuals could be removed and summary statistics regenerated or the meta-analysis

‡90 analysis itself can be adapted to correct for potential correlation due to n_o ²⁸. However, in many
‡91 circumstances, individual cohorts are not permitted to share individual-level data, either by national law or
‡92 by local ethical review board conditions. To get around this problem, Turchin and Hirshhorn¹⁰ created a
‡93 software tool, Gencrypt, which utilizes a security protocol known as one-way cryptographic hashes to allow
‡94 overlapping participants to be identified without sharing individual-level data. To our knowledge, this
‡95 encryption method has yet to be employed in meta-analysis studies. We propose an alternative approach,
‡96 pseudo profile score regression (PPSR), which involves sharing of weighted linear combinations of SNP
‡97 genotypes with the central meta-analysis hub. In essence, multiple random profile scores are generated for
‡98 each individual in each cohort, using SNP weights supplied by the analysis hub, and the resulting scores are
‡99 provided back to the analysis hub. PPSR works through three steps (**Supplementary notes and**
‡00 **Supplementary Fig. 9**), and the purpose of PPSR is to estimate a relationship-like matrix of $n_i \times n_j$
‡01 dimension for a pair of cohorts, which have n_i and n_j individuals respectively. Each entry of the matrix is
‡02 filled with genetic similarity for a pair of samples from each of the two cohorts, estimated via the PPSR.

‡03
‡04 We use WTCCC data as an illustration to detect 2,934 shared controls between any two of the diseases by
‡05 PPSR. Among 330K unambiguous SNPs, which are not palindromic (A/T or G/C alleles), we randomly
‡06 picked $M = 100, 200,$ and 500 SNPs, to generate pseudo profile scores. It generated 21 cohort-pair
‡07 comparisons, leading to the summation for 488,587,090 total individual-pair tests. To have an experiment-
‡08 wise type I error rate = 0.01, type II error rate = 0.05 (power = 0.95) for detecting overlapping individuals,
‡09 we needed to generate at least 57 pseudo profile scores (PPS). We generated scores $S = [s_1, s_2, s_3, \dots, s_{57}]$,
‡10 where each s is a vector of M elements, sampled from a standard normal distribution (**Supplementary**
‡11 **notes**). S is shared across 7 cohorts for generating pseudo-profile scores for each individual. In total 57 PPS
‡12 were generated for each individual in each cohort. For a pair of cohorts, PPSR was conducted for each
‡13 possible pair of individuals for any two cohorts over the generated pseudo-profile scores. Once the
‡14 regression coefficient (b) was greater than the threshold, here $b = 0.95$, the pair of individuals was inferred
‡15 to be having highly similar genotypes, implying that the individual was included in both cohorts
‡16 (**Supplementary notes**).

‡17
‡18 When using 200 and 500 random SNPs, all the known 2,934 shared controls were detected from 21 cohort-
‡19 pair-wise comparison; when using 100 randomly SNPs, on average 2,931 shared samples were identified,
‡20 which is more accurate than using λ_{meta} constructed using either genetic effects or allele frequencies (**Fig.**
‡21 **8b**). In addition, for detected overlapping samples, there were no false positives observed – consistent with
‡22 simulations that show the method was conservative in the controlling type I error rate (**Supplementary**
‡23 **notes**). For comparison, we also used the Gencrypt to detect overlapping samples using the same set of
‡24 SNPs as used in PPSR. Although Gencrypt guidelines suggest use of at least 20,000 random SNPs¹⁰,
‡25 selecting 500 random SNPs in the WTCCC cohorts also provided good accuracy with Gencrypt, and on

‡26 average about 2,920 (99.6% of the shared controls) overlapping samples were detected, only slightly lower
‡27 than PPSR. For example, for BP and CAD, Gencrypt detected 2,912 shared controls, but was unable to
‡28 identify about 20 overlapping controls, due to missing data (on average 1% missing rate). Increasing the
‡29 number of SNPs when using Gencrypt is likely to overcome the problem of missing data.

‡30

‡31 Furthermore, PPSR is able to detect pairs of relatives. For example, between the BD and CAD cohorts, two
‡32 pairs of apparent first-degree relatives were detected (**Fig. 9a**). In order to find additional first-degree
‡33 relatives between BD and CAD cohorts, at least 265 PPS were required to have a type I error rate of 0.01
‡34 and type II error rate of 0.05 (**Supplementary notes**) for a regression coefficient cutoff of 0.45, a threshold
‡35 for first-degree relatives. As expected, all other individuals that did not show high relatedness did not reach
‡36 the threshold of 0.45 of the PPS regression coefficient for first-degree relatives (**Fig. 9b**). Gencrypt did not
‡37 detect any first-degree relatives.

‡38

‡39 The speed of PPSR depends on $n_i \times n_j$, the sample sizes for a pair of cohorts, and the number of PPS for
‡40 each cohort; for the WTCCC data there are 21 cohort-pair comparisons, and each pair took about 20 minutes,
‡41 on a computer with a 2.3 GHz CPU, given about $5,000 \times 5,000 = 25,000,000$ comparisons. The average
‡42 sample size of GIANT is about 1,500, and takes about 2 minutes for each pair of cohorts. The two largest
‡43 datasets are deCODE with 26,790 samples and WGHS with 23,100 samples, and PPSR to detect overlapping
‡44 samples takes about 8.5 hours. As each pair of individuals is computationally an independent unit, analysis
‡45 jobs can be parallelized on a cluster. Therefore, even for meta-analyses involving many large cohorts, the
‡46 computation time is not a limiting factor.

‡47

‡48 PPSR for each individual uses very little personal information and can be minimized so that there is very
‡49 low probability of decoding it. One way to attempt to decode the genotypes from PPS is to reverse the PPSR,
‡50 so that the individual genotypes can be predicted in the regression (**Supplementary notes**). The individual-
‡51 level genotypic information that can be recovered by an analyst, who knows the S matrix (the weights for
‡52 generating PPS), is determined by the ratio between the number of markers (M) that generated PPS and the
‡53 number of PPS (K). Therefore, inferred information on individual genotypes can be minimized and tailored
‡54 to any specific ethics requirements. We suggest $\frac{M}{K} > 5 \sim 10$ to protect the privacy with sufficient accuracy
‡55 (**Fig 9c**). Of note, if a meta-analysis is conducted within a research consortium, the application of PPSR is
‡56 even safer because the exchange of information is between the consortium analysis hub and each cohort
‡57 independently.

‡58

‡59

Discussion

‡60 In this study, we provide a set of metrics for monitoring and improving the quality of large-scale GWAMA
‡61 based on summary statistics. These tools not only enrich the toolkit to analysts for GWAMA, but also

‡62 provide informative summary and visualization for readers to understand the experimental design of
‡63 GWAMA. As far as we know, no GWAMA to date has checked cohort-level outliers based upon population
‡64 differentiation metrics or utilized estimated allelic effect sizes to identify and quantify sample overlap.

‡65

‡66 Using the F_{st} derived genetic distance measure, we can place all cohorts on an inferred geographic map and
‡67 can easily identify cohorts that are genetic outliers or that have unexpected ancestry. In application, we
‡68 should note that the F_{st} measure can identify unusual summary information, such as detected in the MIGEN
‡69 cohorts from GIANT Consortium GWAMAs, in which the same allele frequencies were reported for all
‡70 cohorts. Meta-PCA can also be used to infer the genetic background of cohorts. The high concordance
‡71 between F_{pc} and meta-PCA indicates the both methods are robust. In practice, meta-PCA may be much
‡72 easier to implement when there are many cohorts, such as GIANT height cohorts and MetaboChip BMI
‡73 cohorts, but the coordinates of a cohort may be slightly shifted with inclusion or exclusion of other cohorts.

‡74

‡75 There are limitation for both F_{pc} and meta-PCA. Firstly, the inference depends on the choice of reference
‡76 cohorts. Meta-PCA is further upon the inclusion or exclusion of other cohorts. However, given the
‡77 application of the data, we believe the impact will not influence the inference of the genetic background of
‡78 cohorts in meta-analysis. Secondly, various mechanisms can give the identical projection in PCA¹⁴. The
‡79 purpose of both methods is to find the discordance between demographic information and genetic
‡80 information, or outliers. The projection is not attempt to discover the detailed demographic past that shapes a
‡81 cohort.

‡82

‡83 Our third metric λ_{meta} provides information on sample overlap and heterogeneity between cohorts by
‡84 utilizing the estimated allelic effect sizes and their standard errors. In most meta-analyses, the overall λ_{meta}
‡85 is likely to be slightly greater than 1 solely due to unknown heterogeneity, slight as observed, in generating
‡86 the phenotype and genotype data that cannot be accounted for by QC. The observed mean of λ_{meta} for the
‡87 GIANT height GWAMA was 1.03 but with more variation than expected by chance. The strong correlation
‡88 between λ_{GC} and λ_{meta} indicated the reported sampling of the reported data were systematically driven by
‡89 analysis protocols. For cohorts with $\lambda_{GC} < 1$ and $\lambda_{meta} < 1$, it is likely that the GWAS modeling strategy
‡90 employed for GWAS in the cohort was too conservative, for example MIGEN cohorts might have on
‡91 average too small sample size for each cohort. Conversely, for cohorts with $\lambda_{GC} > 1$ and $\lambda_{meta} > 1$ results
‡92 are too heterogeneous, perhaps reflecting systematically smaller sampling variances of the reported genetic
‡93 effects. As the GWAMA often uses inverse-variance-weighted meta-analysis²⁵, such cohorts may lead to
‡94 incorrect weights to the different cohorts in the meta-analysis, suggesting that the statistical analysis in meta-
‡95 analyses can be improved by applying better weighting factors.

‡96

i97 It is well-recognised that overlapping samples may inflate the type-I error rate of GWAMA and therefore
i98 lead to false positives. Although post-hoc correction of the test statistic is possible^{26–28}, stringent quality
i99 control ruling out overlapping samples makes the whole analysis easier and lowers the risk of false positives.
i00 A better solution would be to rule out shared samples at the start, for pairs of cohorts that show deflated
i01 λ_{meta} , and we propose PPSR to accomplish this.

i02

i03 In summary, to maximize the inference from multi-cohort GWAMA, accurate cohort-level information on
i04 allele frequencies, estimated effect sizes, and their sampling variance can be exploited to perform additional
i05 measures that are likely to lead to reduction in the number of false positives and increasing statistical power
i06 for gene discovery. All methods proposed are implemented in freely available software GEAR.

i07

i08 **Acknowledgements**

i09 This work was funded by Australian National Health and Medical Research Council Project and Fellowship
i10 grants (1011506, 613601, 613602, 1078901, 1078037), grants GM 099568 from the National Institutes of
i11 Health and the Sylvia & Charles Viertel Charitable Foundation. This study makes use of data generated by
i12 the Wellcome Trust Case-Control Consortium. A full list of the investigators who contributed to the
i13 generation of the data is available from www.wtccc.org.uk. We also thank from High Performing
i14 Computing support from the Information Technology group at the Queensland Brain Institute, The
i15 University of Queensland.

i16

i17 **Author contributions:**

i18 GBC and PMV designed the study. GBC, PMV and SHL derived the analytical results. GBC performed all
i19 analysis. CGB and ZZZ developed the software. GBC and PMV wrote the first draft of the paper. MRR, JY,
i20 NW discussed results and methods, and provided comments that improved earlier versions of the manuscript.
i21 Other authors provided cohort-level summary statistics and contributed to improving the study and
i22 manuscript.

i23

i24 **Competing financial interests:**

i25 The authors declare no competing financial interests.

i26

i27 **Web resources:**

i28 GEAR (GEnetic Analysis Repository): <http://www.complextraitgenomics.com/>

i29 PGC: <http://www.med.unc.edu/pgc/results>

i30 1000 Genomes Project: <http://www.1000genomes.org/>

i31

32 References

- 33 1 Visscher PM, Brown M a, McCarthy MI, Yang J. Five years of GWAS discovery. *Am J Hum Genet*
34 2012; **90**: 7–24.
- 35 2 Winkler TW, Day FR, Croteau-Chonka DC, Wood AR, Locke AE, Mägi R *et al.* Quality control and
36 conduct of genome-wide association meta-analyses. *Nat Protoc* 2014; **9**: 1192–212.
- 37 3 Wood AR, Esko T, Yang J, Vedantam S, Pers TH, Gustafsson S *et al.* Defining the role of common
38 variation in the genomic and biological architecture of adult human height. *Nat Genet* 2014; **46**:
39 1173–1186.
- 40 4 Locke AE, Kahali B, Berndt SI, Justice AE, Pers TH, Day FR *et al.* Genetic studies of body mass
41 index yield new insights for obesity biology. *Nature* 2015; **518**: 197–206.
- 42 5 Voight BF, Kang HM, Ding J, Palmer CD, Sidore C, Chines PS *et al.* The Metabochip, a custom
43 genotyping array for genetic studies of metabolic, cardiovascular, and anthropometric traits.
44 *PLoS Genet* 2012; **8**: e1002793.
- 45 6 The 1000 Genomes Project Consortium. An integrated map of genetic variation from 1,092
46 human genomes. *Nature* 2012; **491**: 56–65.
- 47 7 The Wellcome Trust Case Control Consortium. Genome-wide association study of 14,000 cases
48 of seven common diseases and 3,000 shared controls. *Nature* 2007; **447**: 661–678.
- 49 8 Purcell S, Neale B, Todd-Brown K, Thomas L, Ferreira M a R, Bender D *et al.* PLINK: a tool set for
50 whole-genome association and population-based linkage analyses. *Am J Hum Genet* 2007; **81**:
51 559–75.
- 52 9 Devlin B, Roeder K. Genomic control for association studies. *Biometrics* 1999; **55**: 997–1004.
- 53 10 Turchin MC, Hirschhorn JN. Gcrypt: one-way cryptographic hashes to detect overlapping
54 individuals across samples. *Bioinformatics* 2012; **28**: 886–8.
- 55 11 Novembre J, Johnson T, Bryc K, Kutalik Z, Boyko AR, Auton A *et al.* Genes mirror geography
56 within Europe. *Nature* 2008; **456**: 98–101.
- 57 12 Cavalli-Sforza LL, Menozzi P, Piazza A. *The History and Geography of Human Genes*. Princeton
58 University Press, 1996.
- 59 13 Patterson N, Price AL, Reich D. Population structure and eigenanalysis. *PLoS Genet* 2006; **2**:
60 e190.
- 61 14 McVean G. A genealogical interpretation of principal components analysis. *PLoS Genet* 2009; **5**:
62 e1000686.
- 63 15 Bryc K, Bryc W, Silverstein JW. Separation of the largest eigenvalues in eigenanalysis of
64 genotype data from discrete subpopulations. *Theor Popul Biol* 2013; **89**: 34–43.
- 65 16 Chaput J-P, Pérusse L, Després J-P, Tremblay A, Bouchard C. Findings from the Quebec Family
66 Study on the Etiology of Obesity: Genetics and Environmental Highlights. *Curr Obes Rep* 2014; **3**:
67 54–66.
- 68 17 Diabetes Genetics Initiatives. Genome-wide association analysis identifies loci for type 2
69 diabetes and triglyceride levels. *Science (80-)* 2007; **316**: 1331–1336.
- 70 18 Igl W, Johansson A, Gyllensten U. The Northern Swedish Population Health Study (NSPHS)--a
71 paradigmatic study in a rural population combining community health and basic research. *Rural*
72 *Remote Health* 2010; **11**: 1363.
- 73 19 de Bakker PIW, Ferreira M a R, Jia X, Neale BM, Raychaudhuri S, Voight BF. Practical aspects of
74 imputation-driven meta-analysis of genome-wide association studies. *Hum Mol Genet* 2008; **17**:
75 R122–8.
- 76 20 Ripke S, Sanders AR, Kendler KS, Levinson DF, Sklar P, Holmans P a *et al.* Genome-wide
77 association study identifies five new schizophrenia loci. *Nat Genet* 2011; **43**: 969–76.
- 78 21 Ripke S, O'Dushlaine C, Chambert K, Moran JL, Kähler AK, Akterin S *et al.* Genome-wide
79 association analysis identifies 13 new risk loci for schizophrenia. *Nat Genet* 2013; **45**: 1150–9.
- 80 22 Okada Y, Wu D, Trynka G, Raj T, Terao C, Ikari K *et al.* Genetics of rheumatoid arthritis
81 contributes to biology and drug discovery. *Nature* 2014; **506**: 376–381.
- 82 23 Calò C, Melis A, Vona G, Piras I. Sardinian Population (Italy): a Genetic Review. *Int J Mod*
83 *Anthropol* 2010; **1**: 39–64.
- 84

- i85 24 Yang J, Weedon MN, Purcell S, Lettre G, Estrada K, Willer CJ *et al.* Genomic inflation factors
i86 under polygenic inheritance. *Eur J Hum Genet* 2011; **19**: 807–12.
- i87 25 Willer CJ, Li Y, Abecasis GR. METAL: fast and efficient meta-analysis of genomewide association
i88 scans. *Bioinformatics* 2010; **26**: 2190–1.
- i89 26 Bolormaa S, Pryce JE, Reverter A, Zhang Y, Barendse W, Kemper K *et al.* A multi-trait, meta-
i90 analysis for detecting pleiotropic polymorphisms for stature, fatness and reproduction in beef
i91 cattle. *PLoS Genet* 2014; **10**: e1004198.
- i92 27 Zhu X, Feng T, Tayo BO, Liang J, Young JH, Franceschini N *et al.* Meta-analysis of Correlated
i93 Traits via Summary Statistics from GWASs with an Application in Hypertension. *Am J Hum Genet*
i94 2015; **96**: 21–36.
- i95 28 Lin D-Y, Sullivan PF. Meta-analysis of genome-wide association studies with overlapping
i96 subjects. *Am J Hum Genet* 2009; **85**: 862–72.
- i97
- i98

Figures & Tables

i99

i00 **Figure 1 Recovery of cohort-level genetic background and inference of their geographic locations for**
i01 **GIANT BMI MetaboChip cohorts using the F_{st} derived genetic distance measure.**

i02

i03 **Figure 2 Using the genetic distance spectrum to infer the geographic origins for GIANT height GWAS**
i04 **cohorts.**

i05

i06 **Figure 3 Comparison between Meta-PCA and genotype PCA on 1KG.**

i07

i08 **Figure 4 Recovery of cohort-level genetic background for GIANT BMI MetaboChip cohorts using**
i09 **meta-PCA.**

i10

i11 **Figure 5 The recovery of cohort-level genetic background using meta-PCA analysis for GWAS height**
i12 **cohorts.**

i13

i14 **Figure 6 λ_{meta} for the GIANT height GWAS cohorts.**

i15

i16 **Figure 7 $\bar{\lambda}_{meta}$ and λ_{gc} for GIANT height GWAS cohorts.**

i17

i18 **Figure 8 Pseudo profile score regression for the WTCCC 7 diseases.**

i19

i20 **Figure 9 PPSR coefficients for identifying shared controls/relatives between WTCCC BD and CAD**
i21 **cohorts.**

i22

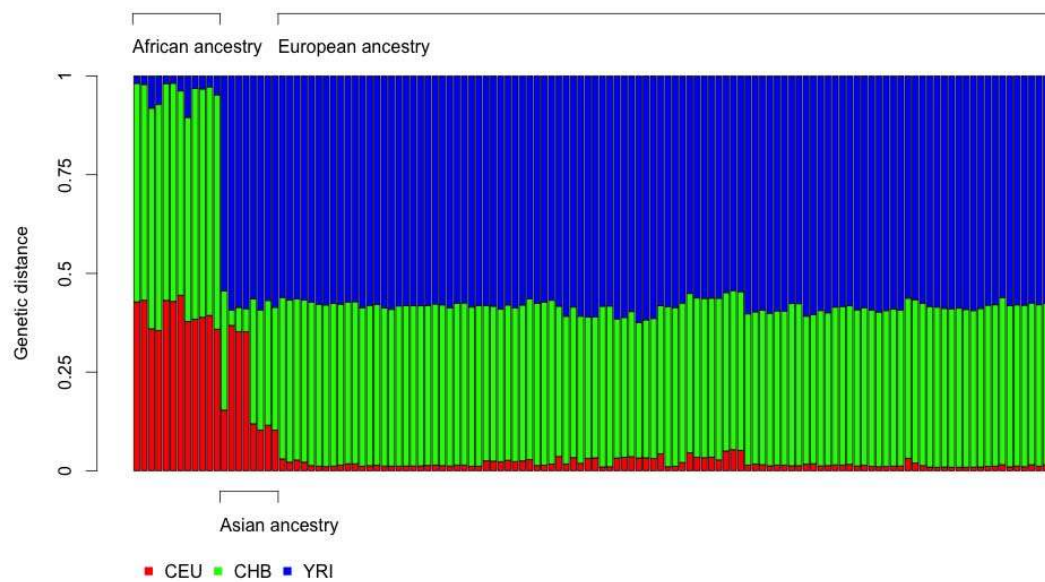
i23 **Table 1 The estimated correlation for a pair of cohorts via their summary statistics**

i24

i25

i26 **Figure 1 Recovery of cohort-level genetic background and inference of their geographic locations for**
i27 **GIANT BMI MetaboChip cohorts using the F_{st} derived genetic distance measure. (a)** Genetic distance
i28 spectrum for all MetaboChip cohorts to CEU, CHB and YRI. See Supplementary notes for more details. The
i29 origins of the cohorts are denoted on the horizontal axis. **(b)** Projection for MetaboChip cohort into F_{PC} space
i30 defined by YRI, CHB, and CEU reference populations. The x- and y-axis represent relative distances
i31 derived from the genetic distance spectrum. Three dashed lines, blue for CEU, green for CHB, and red for
i32 YRI, partitioned the whole F_{PC} space to three genealogical subspaces. **(c)** The genetic distance spectrum for
i33 MetaboChip European cohorts to CEU – Northwest Europeans, FIN – Northeast European, and TSI –
i34 Southern Europeans. The nationality of the cohorts are denoted on the horizontal axis. **(d)** The projection for
i35 MetaboChip European cohorts to the F_{PC} space defined by CEU, FIN, and TSI reference populations. The
i36 whole space is further partitioned into three subspaces, CEU-TSI genealogical subspace (red and blue
i37 dashed lines), FIN-TSI genealogical subspace (green-blue dashed lines), and CEU-FIN genealogical
i38 subspace (red-green dashed lines), respectively. The open circles represent the mean of inferred geographic
i39 locations for the cohorts from the same country. Cohort/country codes: AF, African; AU, Australia; DE,
i40 Germany; EE, Estonia; EU, European Nations; FI, Finland; FIN, Fins in 1000 Genomes Project (1KG); FR,
i41 France; GBR, British in 1KG; GIB, Gujarati Indian in 1KG; GR, Greece; Hawaii, Hawaii in USA; IBS,
i42 Iberian Population in Spain in 1KG; IT, Italy; JM, Jamaica; JPT, Japanese in 1KG; LWK, Luhya in 1KG;
i43 NO, Norway; PH, the Philippines; PK, Pakistan; SC, Seychelles; SCT, Scotland; SE, Sweden; TSI, Tuscany
i44 in 1KG; UK, United Kingdom; US, United States of America.
i45

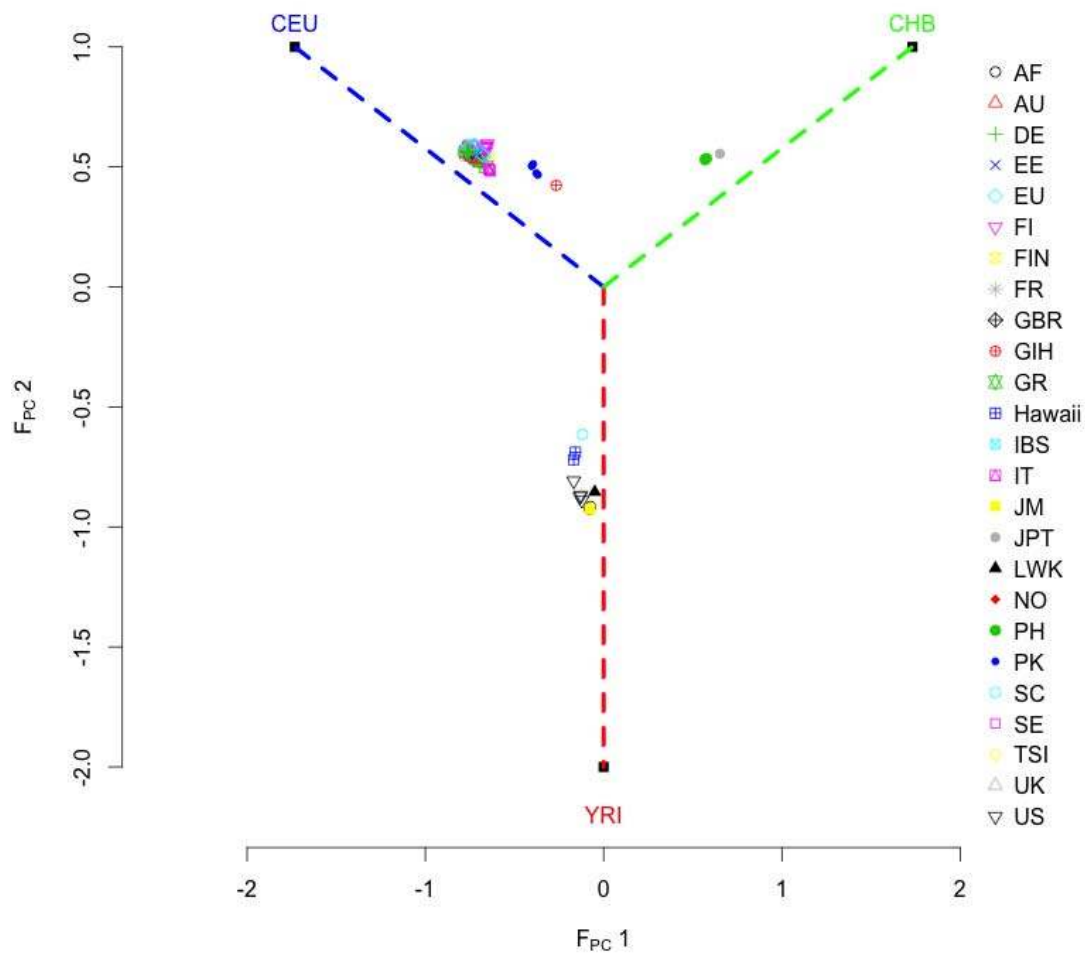
i46 a)



i47

i48

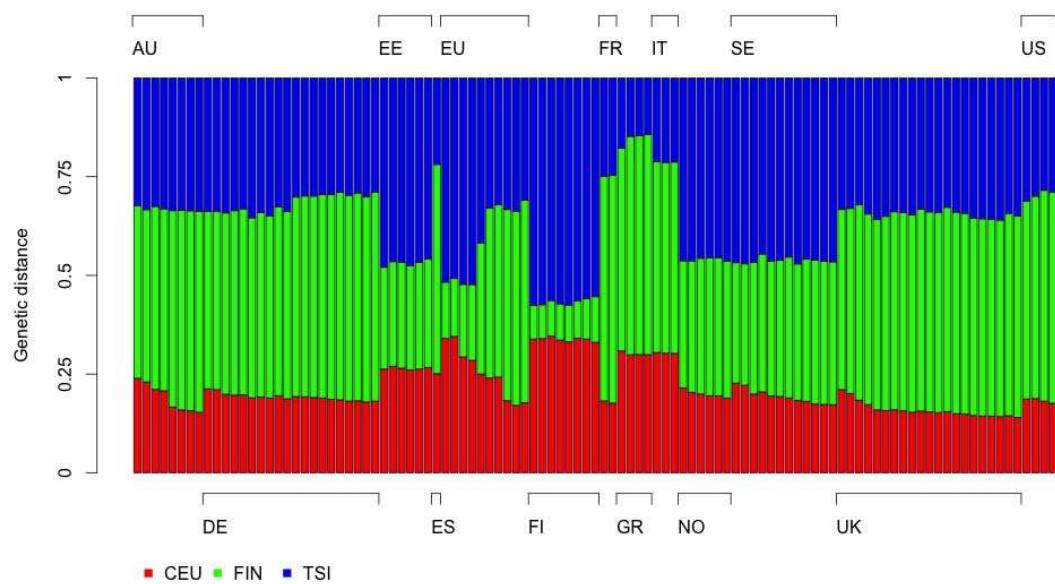
i49 b)



i50

i51

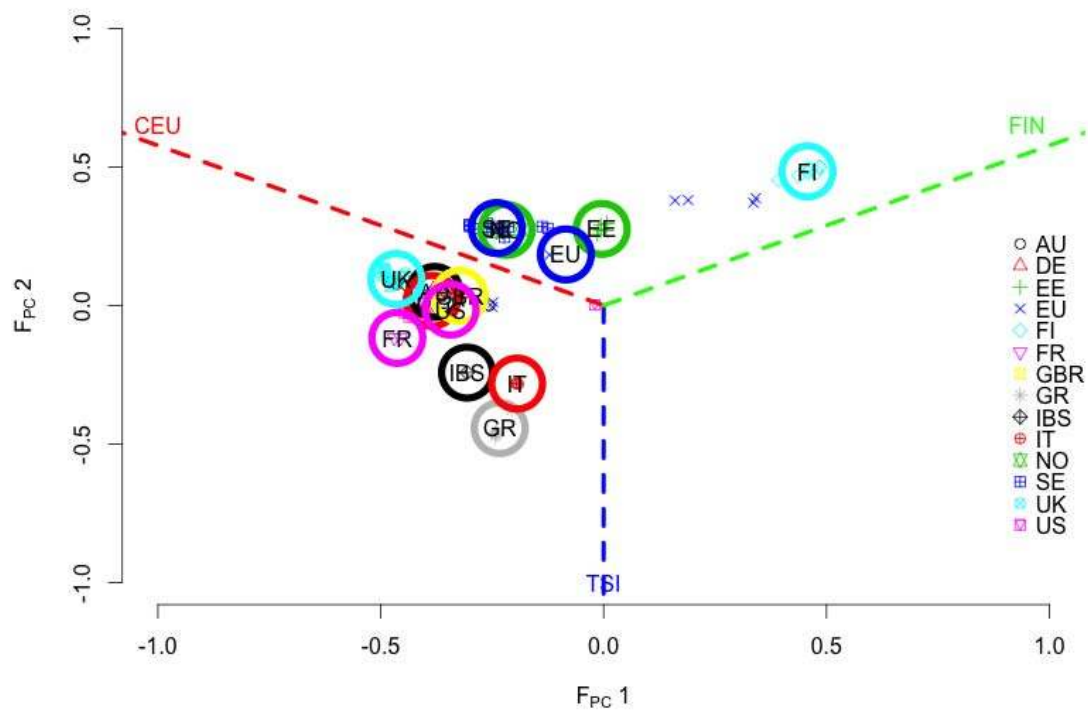
i52 c)



i53

i54

i55 d)

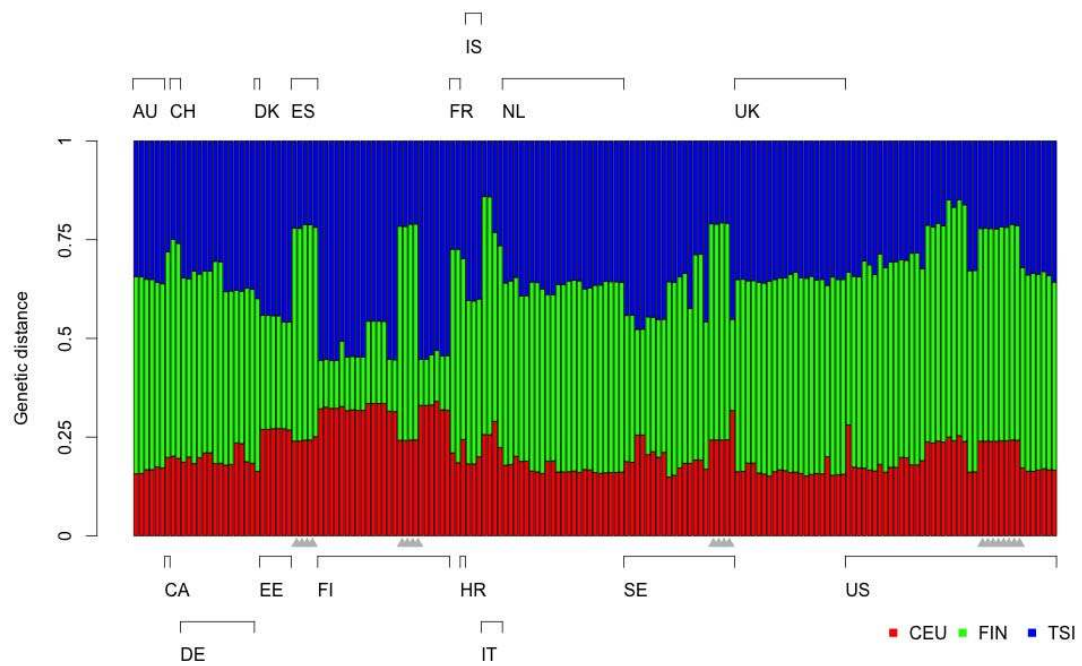


i56

i57

58 **Figure 2 Using the genetic distance spectrum to infer the geographic origins for GIANT height GWAS**
59 **cohorts. (a)** Each cohort has three F_{st} values by comparing with CEU, FIN, and TSI reference samples. The
60 height of each bar represents its relative genetic distance to these three reference populations. The
61 nationalities of the cohorts were denoted along the horizontal axis. The grey triangles along the x-axis
62 indicate MIGEN cohorts. **(b)** Given the three F_{st} values, the location of each cohort can be mapped. The
63 whole space was partitioned into three subspaces, CEU-TSI genealogical subspace (red and blue dashed
64 lines), FIN-TSI genealogical subspace (green and blue dashed lines), and CEU-FIN genealogical subspace
65 (red and green dashed lines). DGI (in the blue box) had samples from the Botnia study. Across MIGEN
66 cohorts (denoted as red triangles in the red box), the same allele frequencies (likely calculated from a South
67 European cohort) were presented for each cohort. Cohort/country codes: AU, Australia; CA, Canada; CH,
68 Switzerland; DE, Germany; DK, Denmark; EE, Estonia; ES, Iberian Population in Spain in 1KG; FI,
69 Finland; FR, France; GR, Greece; IT, Italy; IS, Iceland; NL, Netherlands; SE, Sweden; UK, United
70 Kingdom; US, United States of America.
71

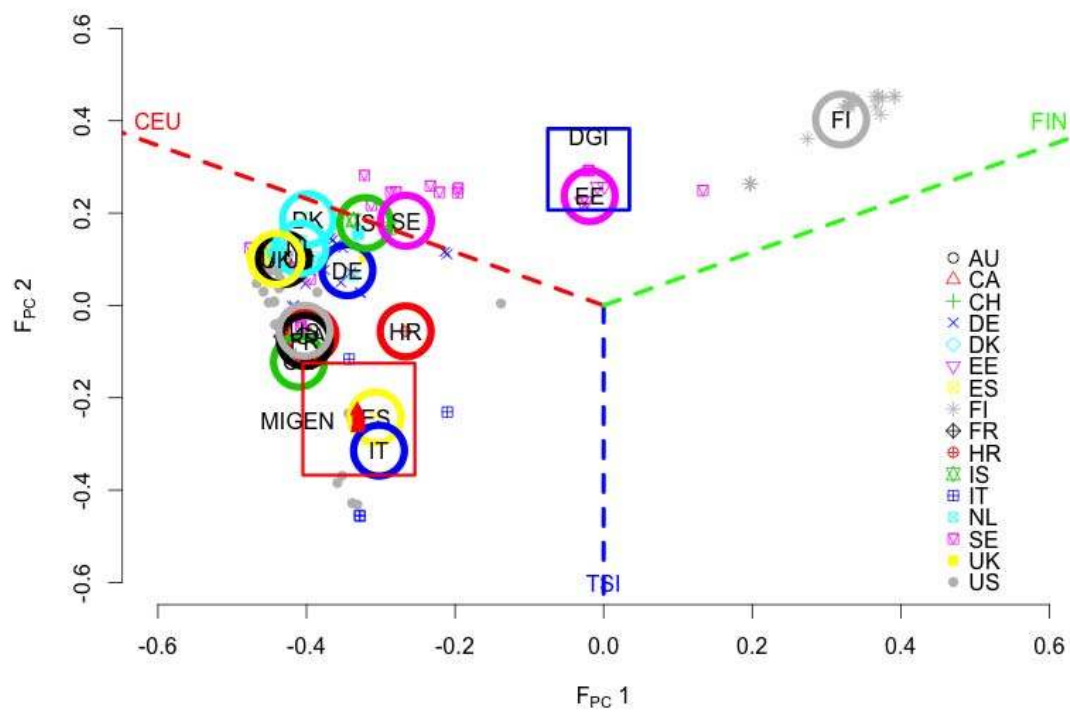
172 a)



173

174

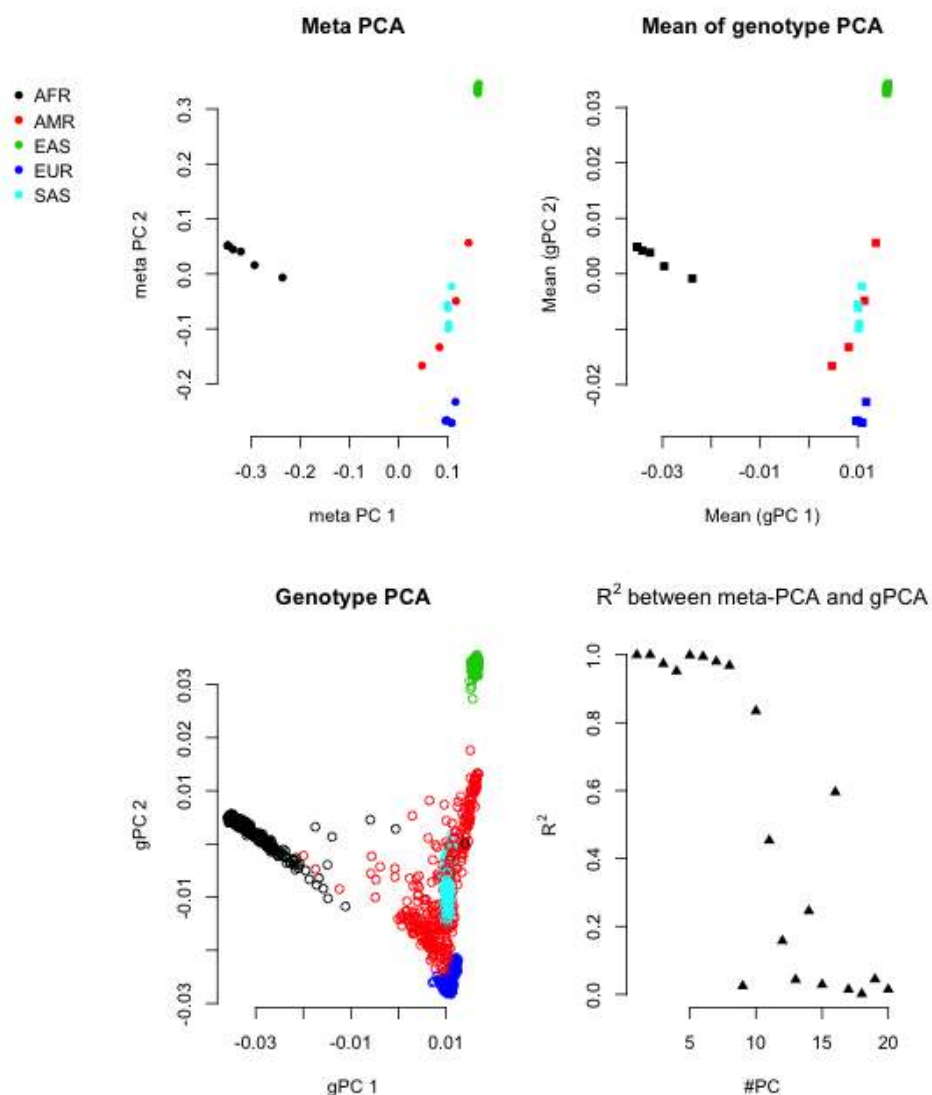
175 b)



176

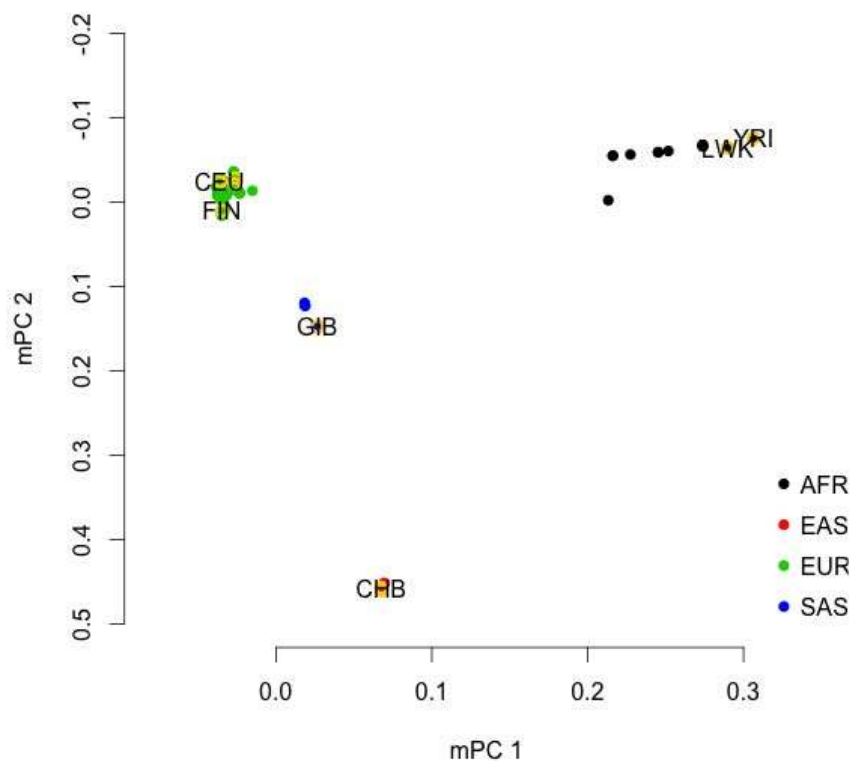
177

i78 **Figure 3 Comparison between Meta-PCA and genotype PCA on 1KG.** Top left panel is the projection of
i79 cohorts based on cohort-level allele frequency for 1KG samples on the first two eigenvectors. Bottom left
i80 panel is conventional PCA based on individual genotypes on the first two eigenvectors. Top right panel is
i81 the projection by taking the mean of the 1KG individuals within each cohort. Bottom right panel is the
i82 correlation, measured in R^2 , between meta-PCA and genotype PCA for the first twenty eigenvectors.



i83
i84

i85 **Figure 4 Recovery of cohort-level genetic background for GIANT BMI Metabochip cohorts using**
i86 **meta-PCA.** The x-axis and y-axis represent the first two eigenvectors from meta-PCA. In meta-PCA,
i87 Metabochip cohorts could be classified into African ancestry (AFR), European ancestry (EUR), East Asian
i88 Ancestry (EAS), and South Asian Ancestry (SAS). The 1KG cohorts, yellow open circles, were added for
i89 comparison.



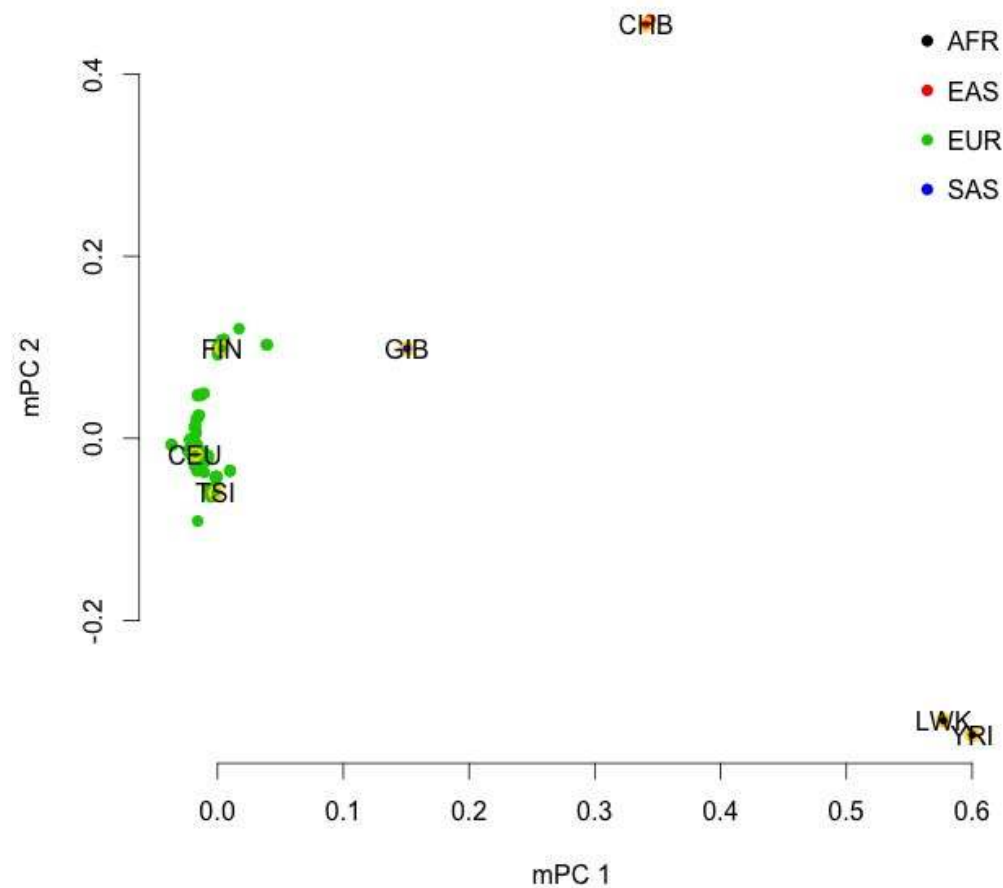
i90
i91
i92

i93 **Figure 5 The recovery of cohort-level genetic background using meta-PCA analysis for GWAS height**
i94 **cohorts.** The x-axis and y-axis represent the first two eigenvectors inferred from meta-PCA. a) The genetic
i95 background inferred with the inclusion of 10 KIG reference populations. b) The genetic background and
i96 relative geographic location for 174 GIANT height cohorts. The large plot on top left was an overview of
i97 174 cohorts, and the rest of plots were classified by the reported demographic information of cohorts. Within
i98 each country-level plot, the small black points represent one cohort, and the large open circle the mean
i99 coordinates for those cohorts from the same country.

'00

'01

a



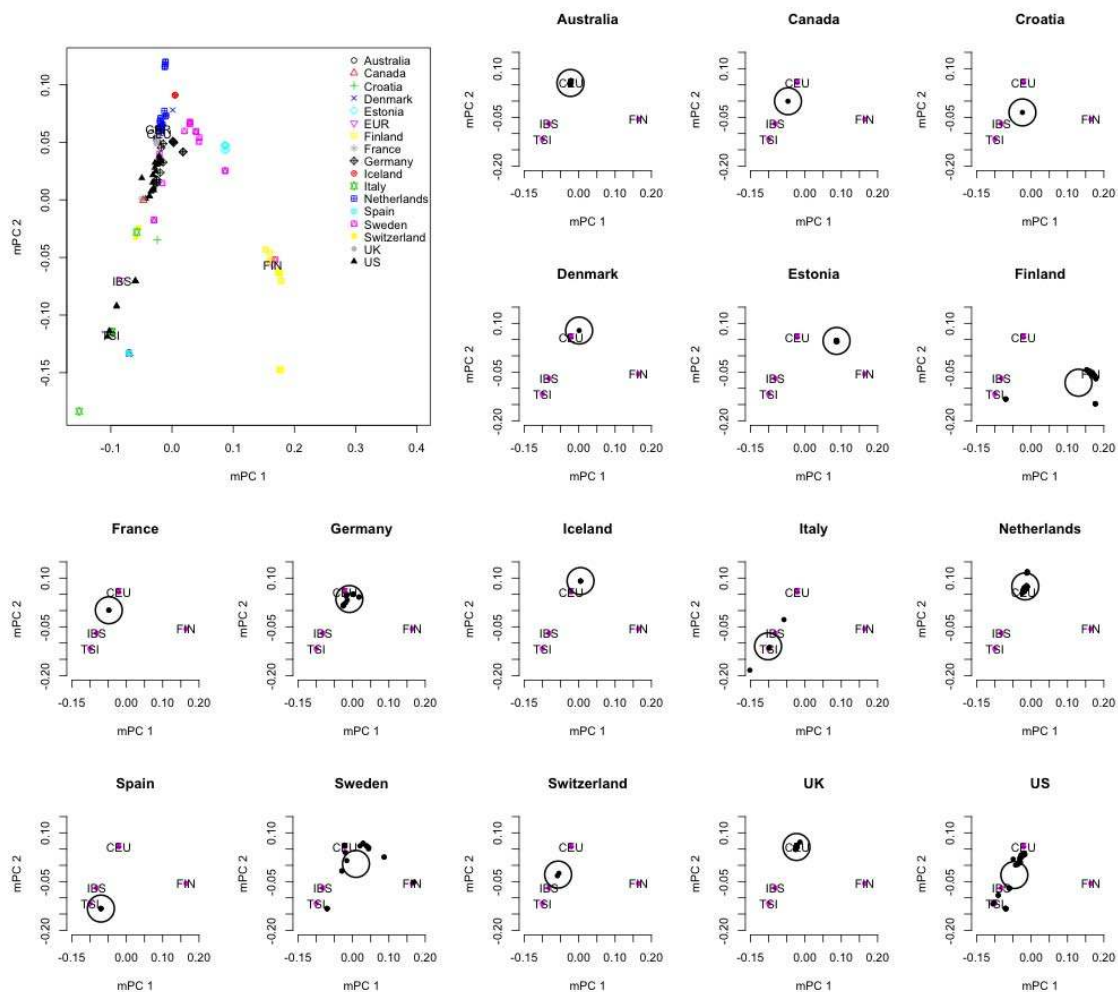
'02

'03

'04

'05

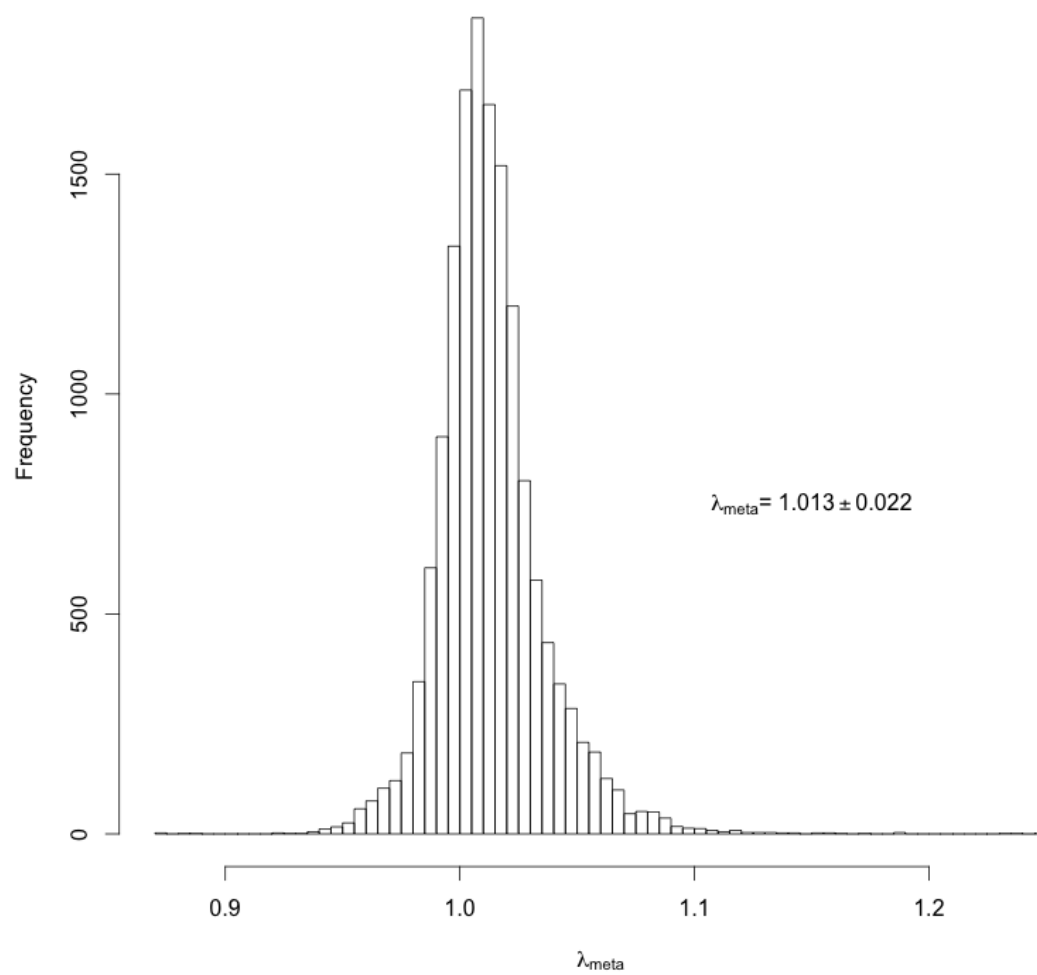
b



'06
'07
'08

'09 **Figure 6 λ_{meta} for the GIANT height GWAS cohorts.** Given 174 cohorts, there are 15,051 λ_{meta} values,
'10 which provide the overview of the quality control of the summary statistics.
'11 **(a)** The distribution of λ_{meta} from 174 cohorts/files used in the GIANT height meta-analysis. The overall
'12 mean of 15,051 λ_{meta} is 1.013, and standard deviation is 0.022. **(b)** The heat map for λ_{meta} . Cohorts
'13 showed heterogeneity ($\lambda_{meta} > 1$) are illustrated on left-top triangle, and homogeneity ($\lambda_{meta} < 1$) on right-
'14 bottom triangle. **(c)** Illustration for homogeneity between two cohorts (SORBS MEN & WOMEN), $\lambda_{meta} =$
'15 0.876. **(d)** Illustration of SARDINIA & WGHS, this pair of cohorts has $\lambda_{meta} = 1.245$. The grey band
'16 represents 95% confidence interval for λ_{meta} .
'17

'18 a)



'19

'20

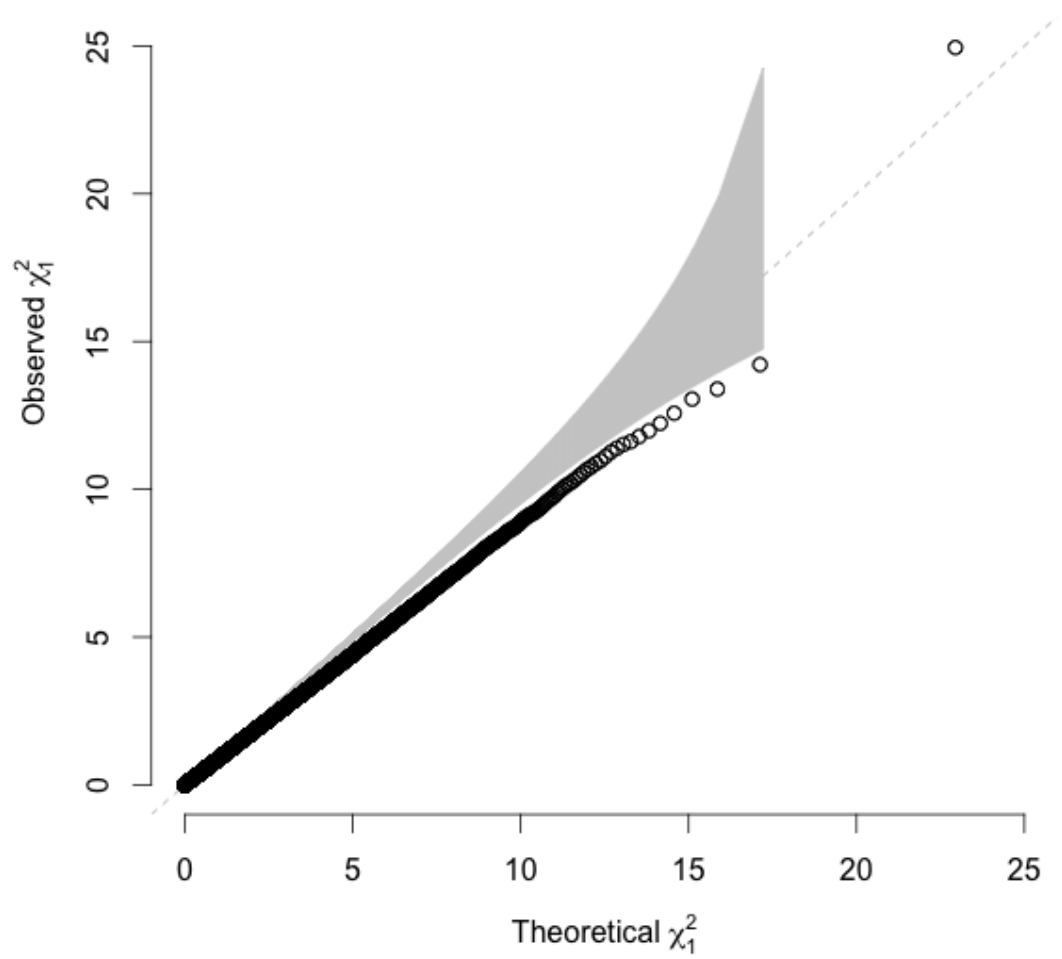
'21 b)



'22

'23

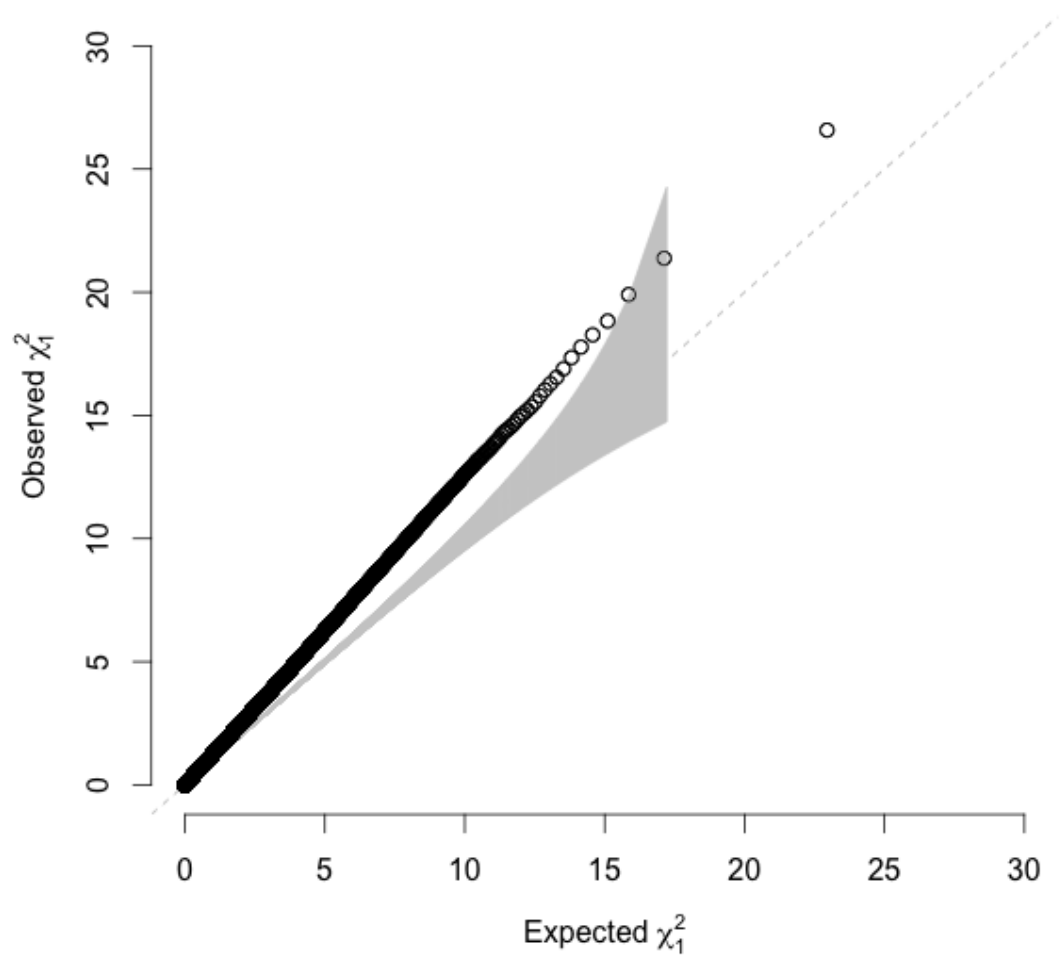
'24 c)



'25

'26

'27 d)

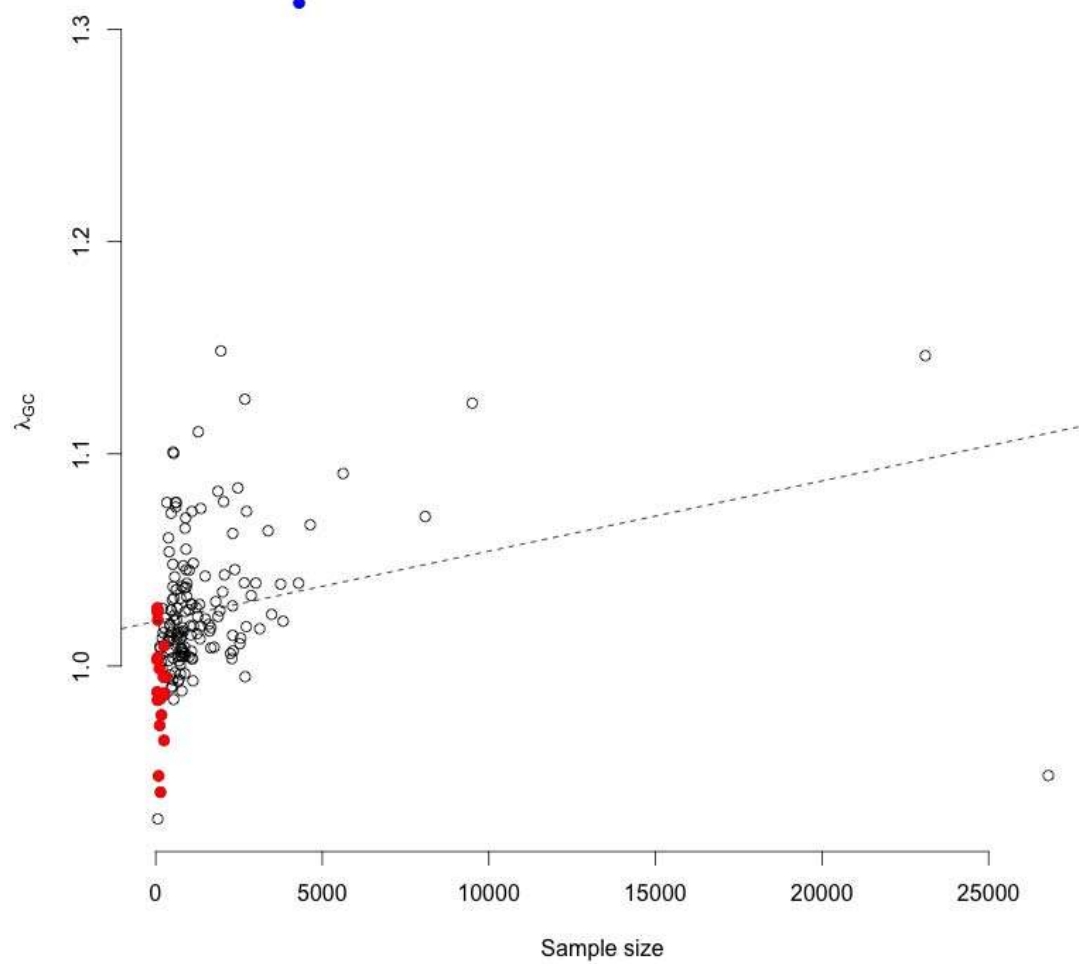


'28

'29

'30 **Figure 7 $\bar{\lambda}_{meta}$ and λ_{gc} for GIANT height GWAS cohorts.** (a) Sample size of each cohort against λ_{GC} .
'31 The linear regression is presented as a dashed line, $\lambda_{GC} = 1.021 + 0.0000033N$, and $R^2 = 0.013$. (b) Sample
'32 size of each cohort against $\bar{\lambda}_{meta}$, which was the mean of a cohort's λ_{meta} over all other cohorts. The linear
'33 regression is presented as a dashed line, $\bar{\lambda}_{meta} = 1.012 + 0.00000055N$ ($N =$ reported sample size), and
'34 $R^2 = 0.055$. (c) λ_{GC} against $\bar{\lambda}_{meta}$ for each cohort, showing a strong correlation, $R^2 = 0.70$. The black dash
'35 line indicates the regression slope for all 174 pairs: $\bar{\lambda}_{meta} = 0.7251 + 0.281\lambda_{GC} + e$. The red dashed line
'36 indicates the regression slope for 20 pairs of MIGEN cohorts: $\bar{\lambda}_{meta} = 0.369 + 0.631\lambda_{GC} + e$. The size of each
'37 circle is proportional to sampling size on logarithm scale. (d) Small sample size leads to a correlation
'38 between $\bar{\lambda}_{meta}$ and λ_{GC} using 174 GIANT height GWAS sample size. 30,000 independent loci, minor allele
'39 frequency ranged from 0.1~0.5, were simulated, and $h^2 = 0.5$. The red dashed line indicates the regression
'40 slope for 20 simulated MIGEN cohorts, $\bar{\lambda}_{meta} = 0.488 + 0.510\lambda_{GC} + e$ ($R^2 = 0.78$). The size of each circle
'41 is proportional to sampling size on logarithm scale. (e) λ_{meta} for whole MIGEN to 174 cohorts. 20 MIGEN
'42 files were combined together to make "whole MIGEN" via meta-analysis, and the summary statistics were
'43 used to calculate λ_{meta} with 174 cohorts using 30,000 independent loci. As MIGEN cohorts were part of
'44 "whole MIGEN", their λ_{meta} were in general below 1. The dashed line is the mean of λ_{meta} of the "whole
'45 MIGEN". The subplot (red box) shows a strong correlation of 0.93 between λ_{meta} (for "whole MIGEN" vs
'46 each MIGEN cohort), and sample size of each MIGEN cohort.
'47

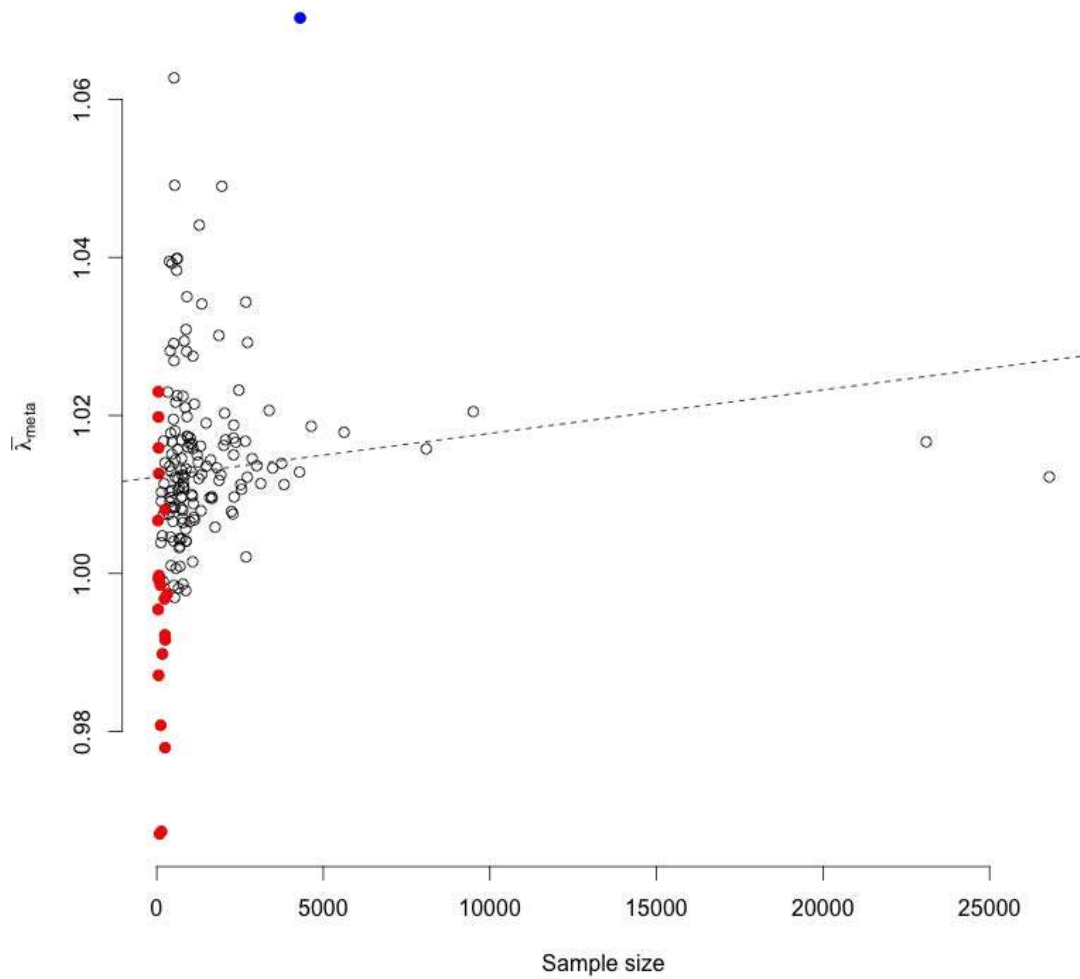
'48 a)



'49

'50

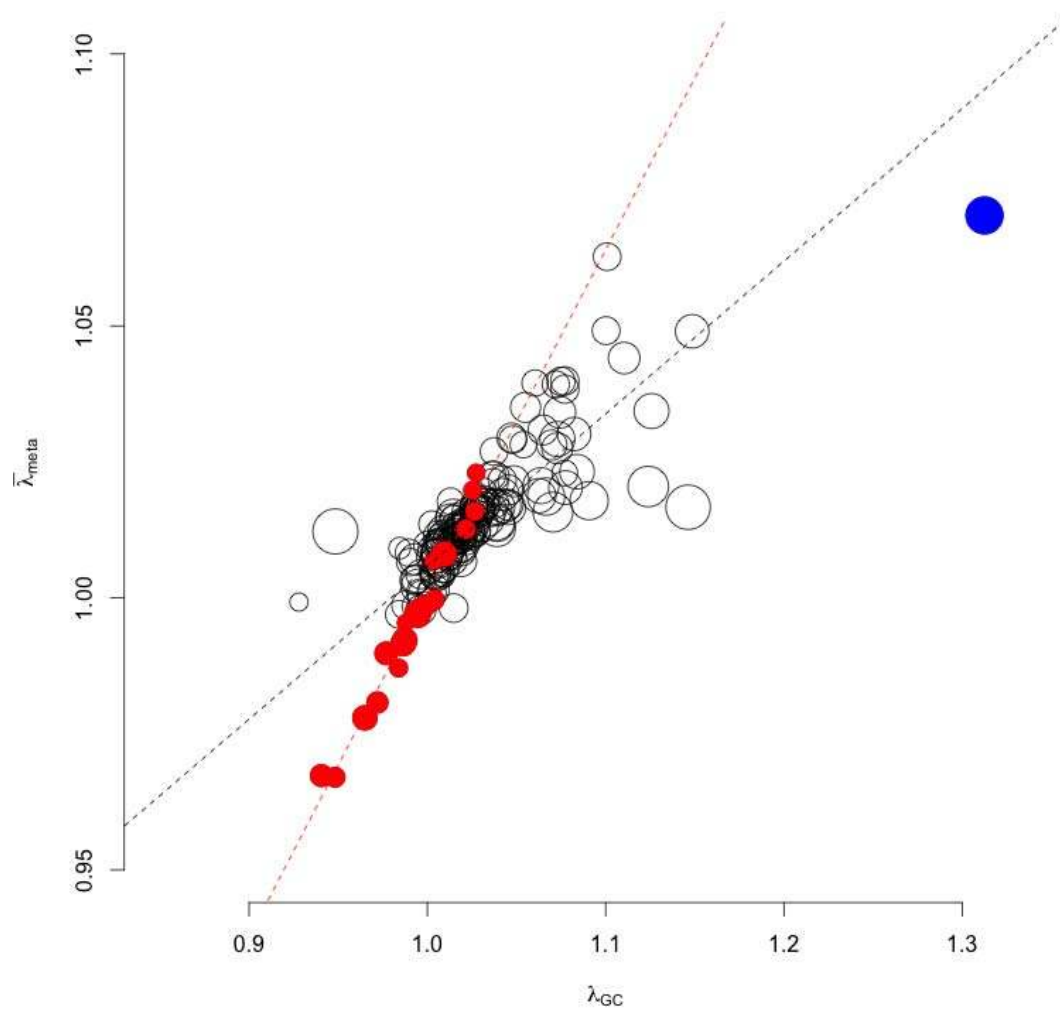
'51 b)



'52

'53

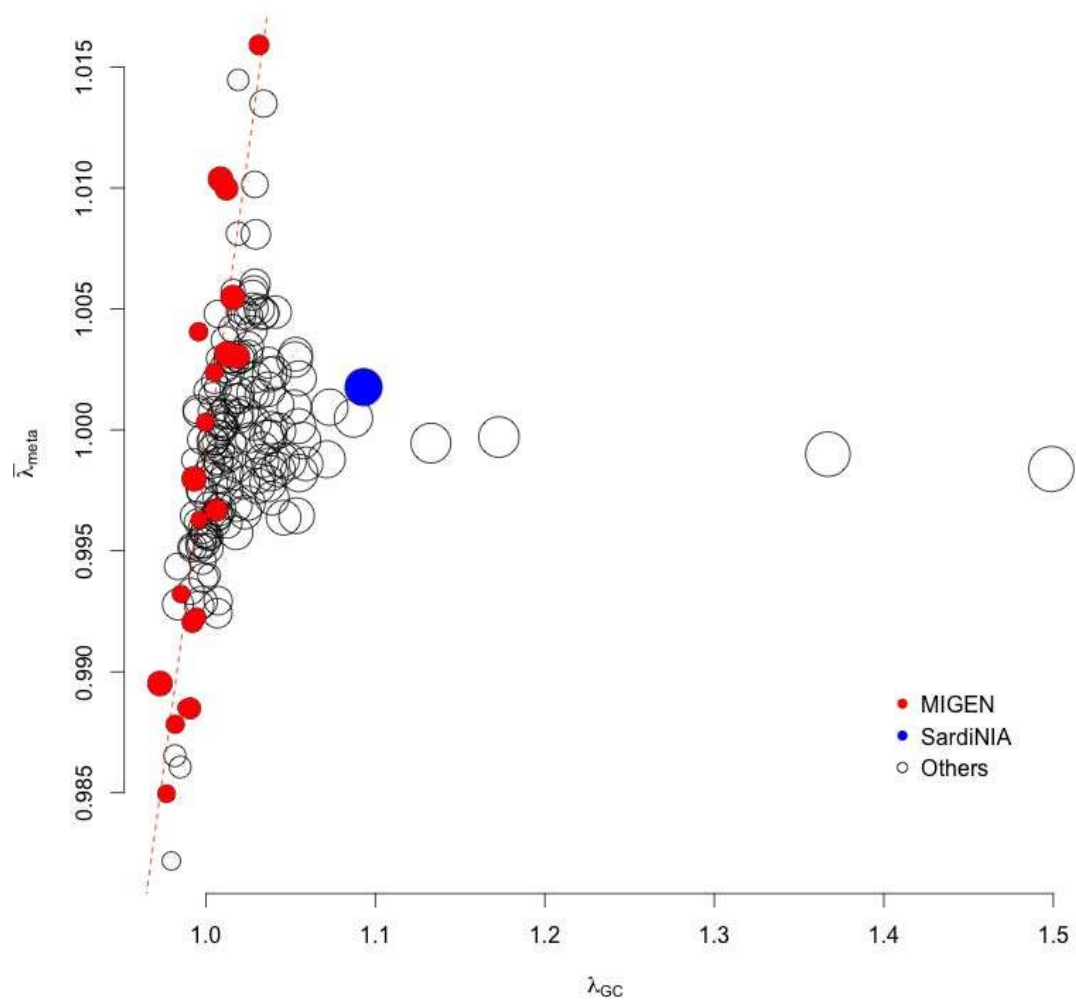
'54 c)



'55

'56

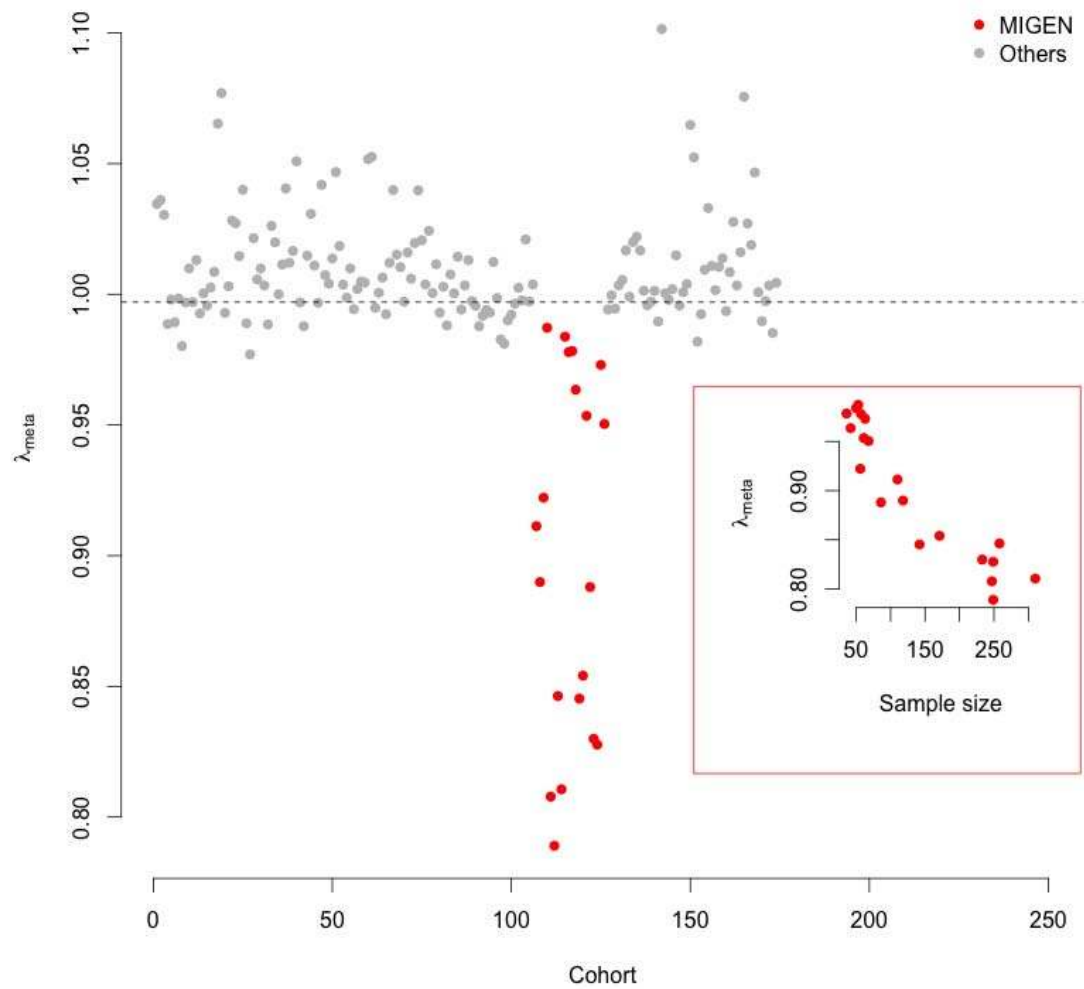
'57 d)



'58

'59

'60 e)

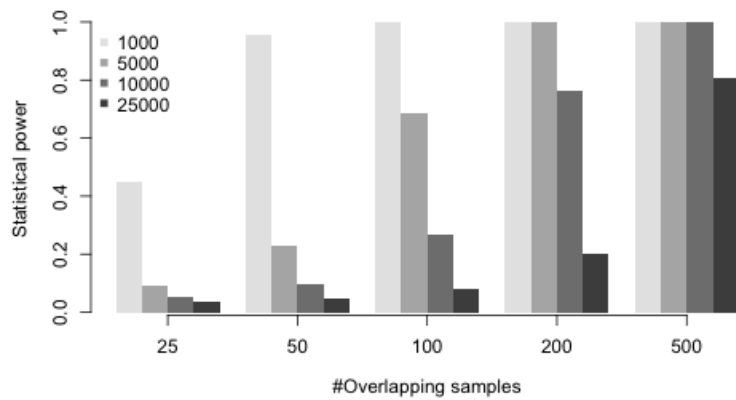


'61

'62

'63 **Figure 8 Pseudo profile score regression for the WTCCC 7 diseases.** a) Statistical power for detecting
'64 overlapping samples between a pair of cohorts given type I error rate of 0.05. Top panel: The y-axis
'65 represents statistical power, and the x-axis the number of overlapping samples. Cohort 1 has 1,000, 5,000,
'66 10,000, or 25,000 samples, and cohort 2 has 1,000 samples. The two cohorts have 25, 50, 100, 200, and 500
'67 overlapping samples. Bottom panel: the corresponding 95% confidence interval is given for each scenario in
'68 the top panel. The statistical power is maximized when the two cohorts have the same sample size. b) Each
'69 cluster represents a pair of cohorts as denoted on the x-axis. Within each cluster, from left to right, the
'70 detected overlapping controls using λ_{meta} based either on effect size estimates or minor allele frequency
'71 (MAF), PPRS using 100, 200, and 500 markers. WTCCC cohort codes: BD for bipolar disorder, CAD for
'72 coronary artery disease, CD for Crohn's disease, HT for hypertension, RA for rheumatoid arthritis, T1D for
'73 type 1 diabetes, T2D for type 2 diabetes.
'74

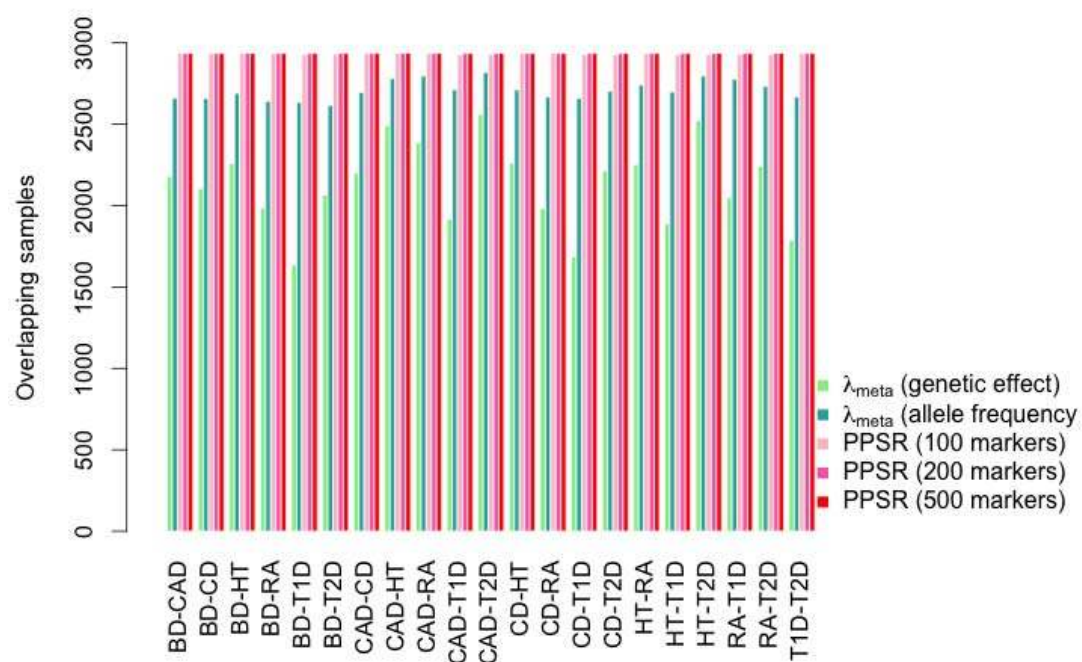
'75 a)



'76

'77

'78 b)

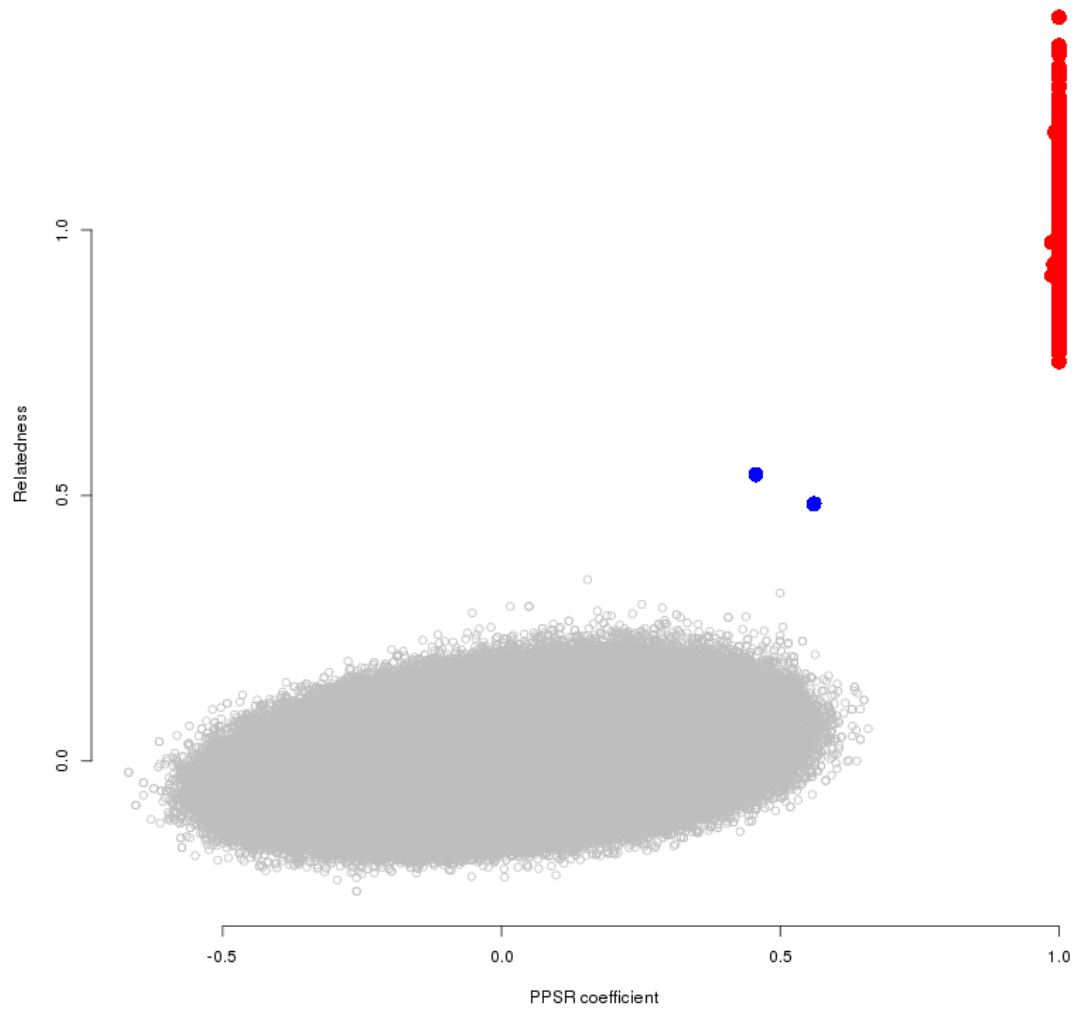


'79

'80

'81 **Figure 9 PPSR coefficients for identifying shared controls/relatives between WTCCC BD and CAD**
'82 **cohorts. (a)** Illustration for regression coefficients between WTCCC BD and CAD from 57 pseudo profile
'83 scores (PPS) generated from 500 markers. The x-axis is the PPSR regression coefficients and y-axis is real
'84 genetic relatedness (as calculated from individual level genotype data). The red points are the shared
'85 controls between two cohorts, and blue points are first-degree relatives. **(b)** The PPS regression coefficients
'86 for detecting overlapping first-degree relatives using 286 PPS generated from 500 markers. **(c)** Decoding
'87 genotypes from the PPS. Given the set of profile scores, one may run a GWAS-like analysis to infer the
'88 genotypes. The ratio between the number of markers (M) and number of pseudo profile scores (K)
'89 determines the potential discovery of individual-level information. The higher the ratio and, the higher the
'90 allele frequency, the less information can be recovered. From left to right, the profile scores generated using
'91 different number of markers. The y-axis is a R^2 metric representing the accuracy between the inferred
'92 genotypes and the real genotypes. From left to right panels 100, 200, 500, and 1000 SNPs were used to
'93 generate 10, 20, 50, and 1000 profiles scores. In each cluster, the three bars are inferred accuracy using
'94 different MAF spectrum alleles, given with the SE of the mean.
'95

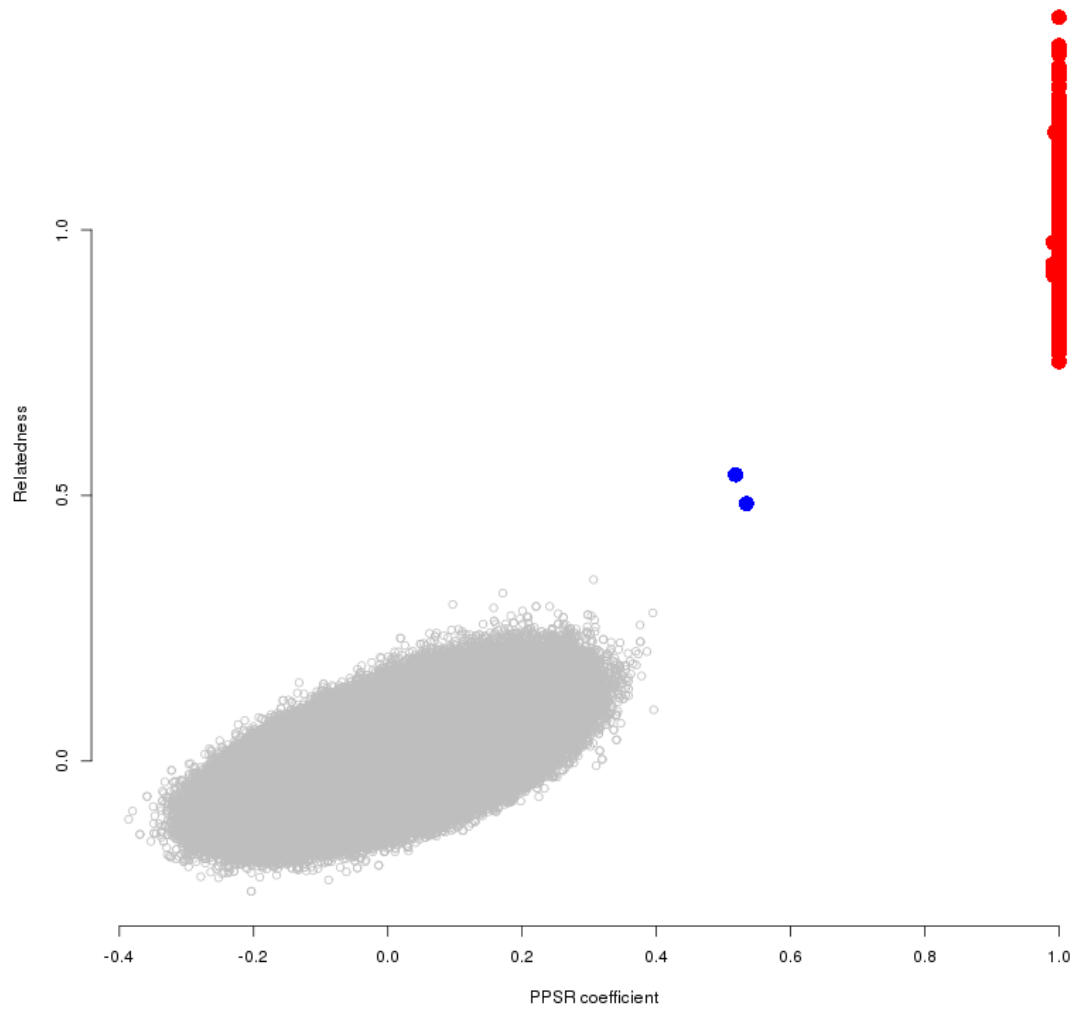
'96 a)



'97

'98

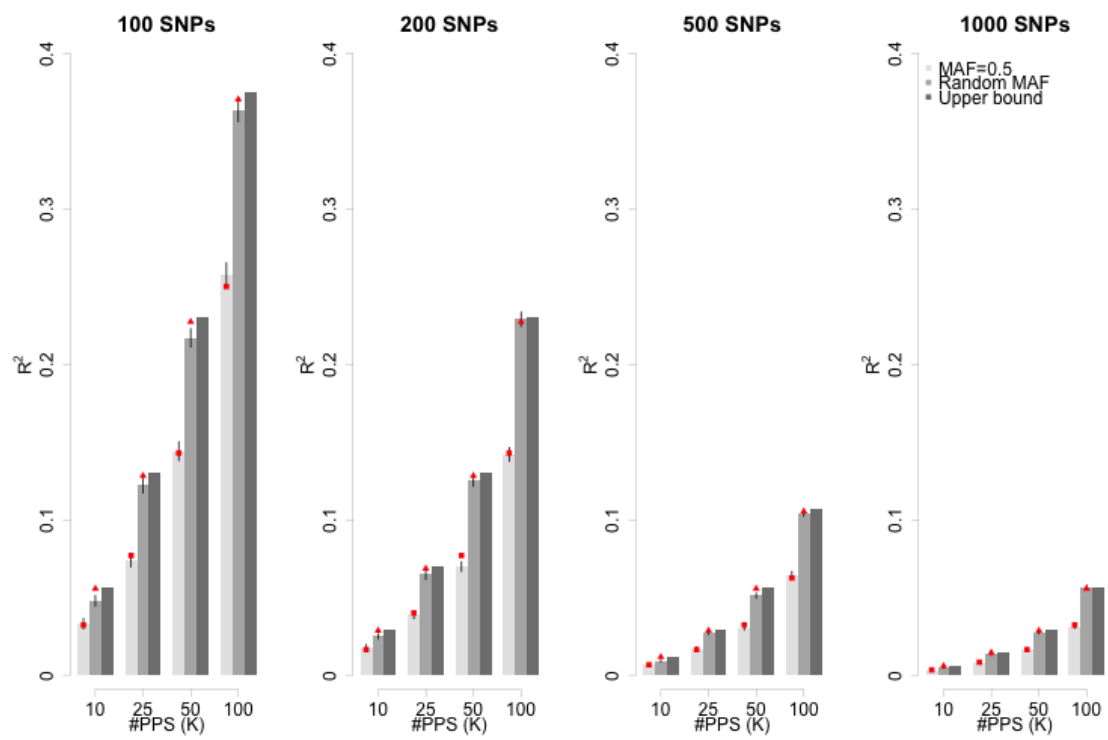
'99 b)



300

301

102 c)



103
104

805 **Table 1 The estimated correlation for a pair of cohorts via their summary statistics**

n_1	n_2	$n_{1,2}$	h^2	M	Q	$\gamma_{1,2} = \frac{n_{1,2}}{\sqrt{n_1 n_2}}$	$\hat{\rho}_{1,2} \pm \text{SD}$	$\hat{\gamma}_{1,2} \pm \text{SD}$
1,000	1,000	100	0.25	30,000	1,000	0.1	0.1072±0.0064	0.101±0.0093
1,000	2,000	100	0.25	30,000	1,000	0.0707	0.0814±0.0054	0.0709±0.0088
1,000	5,000	100	0.25	30,000	1,000	0.0447	0.0615±0.0055	0.0425±0.0096
1,000	10,000	100	0.25	30,000	1,000	0.0316	0.0556±0.0063	0.0325±0.0099
1,000	1,000	1	0.25	30,000	1,000	0.001	0.0092±0.0056	0.0017±0.0093
1,000	2,000	1	0.25	30,000	1,000	0.0007	0.0126±0.0053	0.0006±0.0079
1,000	5,000	1	0.25	30,000	1,000	0.000447	0.0189±0.0060	0.0016±0.0090
1,000	10,000	1	0.25	30,000	1,000	0.000316	0.0259±0.0059	0.0008±0.0092
1,000	1,000	100	0	30,000	1,000	0.1	0.0996±0.0052	0.094±0.0085
1,000	2,000	100	0	30,000	1,000	0.0707	0.0704±0.0048	0.0712±0.0097
1,000	5,000	100	0	30,000	1,000	0.0447	0.0453±0.0057	0.0441±0.0090
1,000	10,000	100	0	30,000	1,000	0.0316	0.0335±0.0057	0.0325±0.0079

806 * Q is the number of QTLs among M simulated loci. We also tried $Q = 100$, the results were nearly identical.

807 $\gamma_{1,2}$ represents the true correlation due to overlapping samples

808 $\hat{\rho}_{1,2}$ represents the estimated correlation estimated via the method proposed by Bolormaa et al²⁶, and Zhu et al²⁷

809 $\hat{\gamma}_{1,2}$ represents the estimated correlation estimate via λ_{meta} , $\hat{\gamma}_{1,2} = \frac{1-\hat{\lambda}_{meta}}{\frac{2\sqrt{n_1 n_2}}{n_1+n_2}}$.

810		Table of contents	
811	Method I: <i>Fst</i> derived genetic distance		51
812	Method II: Principal component analysis for cohort-level allele frequencies		55
813	Method III: The detection of overlapping samples with <i>lambda</i>		56
814	Method IV: Pseudo profile score regression (PPSR).....		61
815			
816			

817 **Method I: F_{st} derived genetic distance**

818 F_{st} is a measure of genetic differentiation between populations. It is usually estimated using
819 individual-level genotype data from multiple samples in two or more populations¹. Here, we
820 calculate F_{st} using summary data on allele frequencies, which implicitly assumes Hardy-
821 Weinberg equilibrium genotype frequencies within populations. We use summary statistic
822 calculated F_{st} as a metric for quality control for each cohort. If the allele frequencies reported
823 for a cohort depart genome-wide from its expectation based on known ancestry due to
824 technical artifacts, then we may observe an unexpected F_{st} value when comparing to a
825 reference panel of known ancestry.

826
827 We calculate F_{st} between each cohort and a reference panel, choosing the appropriate
828 reference sample depending on the purpose of the analysis. For the inference of global-level
829 diversity, we chose YRI, CHB, and CEU as the reference panels. For the inference of within-
830 Europe diversity, we chose CEU, FIN, and TSI as the reference panels. As the different allele
831 frequencies across three samples reflected the real diversity among these reference panels, we
832 did not apply any exclusion criteria on the reference allele frequency. Nevertheless, as
833 GIANT height GWAS samples were imputed to the HapMap panel, the majority of SNPs
834 matched to the 1KG reference samples comprised common SNPs. After ranking the
835 calculated F_{st} in ascending order for all matched SNPs, we sampled 30,000 F_{st} evenly along
836 the ordered F_{st} . These 30,000 markers are quasi-independent and evenly distributed across
837 the genomes. The mean of the 30,000 F_{st} was employed to represent the F_{st} measure between
838 a cohort and a reference panel. The sampled 30,000 markers may differ from one pair of
839 cohorts to another pair, but as tested resample 30,000 markers caused ignorable changes of
840 the mean of F_{st} . Another reason we chose 30,000 markers is that there are around 30,000
841 quasi-independent markers for GWAS data as observed in empirical data and expected from
842 theory^{2,3}.

843
844 In this study, F_{st} is calculated from the allele frequencies estimated from cohorts, provided as
845 summary statistics. F_{st} is treated as a data statistic for measuring allele frequency
846 differentiation. In general the interpretation of F_{st} can vary with context⁴.

$$847 F_{st} = \frac{\frac{r}{(r-1)\sum_{i=1}^r n_i [\sum_{i=1}^r n_i (p_i - \bar{p})^2]}{\bar{p}(1-\bar{p})}} \quad \text{(Equation 1)}$$

848 with p_i the estimated reference allele frequency in population i from a sample of n_i alleles, \bar{p}
849 is the weighted average frequency in the entire sample, and r is the number of populations.

850 Here, we only compared each cohort to the 1KG reference panel, so $r = 2$ and the equation
851 becomes

$$852 \quad F_{st} = \frac{\frac{2}{n_{1,2}}[\sum_{i=1}^2 n_i (p_i - \bar{p})^2]}{\bar{p}(1-\bar{p})} \quad \text{(Equation 2)}$$

853 in which $n_{1,2} = n_1 + n_2$, and $\bar{p} = \frac{n_1}{n_{1,2}}p_1 + \frac{n_2}{n_{1,2}}p_2$ is the mean allele frequency. Alternative
854 estimators for F_{st} are possible, and a comprehensive comparison of different F_{st} estimators
855 was recently reported⁵.

856

857 If the two cohorts are not that different in terms of their allele frequencies, for example, the
858 cohorts from European nations, $p_i \approx p_j \approx \bar{p}$,

$$859 \quad E(F_{st}) \approx \frac{1}{n_{i,j}} + \frac{2n_i n_j [E(p_i) - E(p_j)]^2}{n_{i,j}^2 \bar{p}(1-\bar{p})} \quad \text{(Equation 3)}$$

860 At the right side of the equation, the first term represents the sampling variance for allele
861 frequency for a pair of cohorts, and the second term represents the allele frequency difference
862 due to divergence from a common ancestor. The estimated F_{st} is influenced by sample size,
863 and $F_{st} \geq \frac{1}{n_{i,j}}$, which is the sampling variance of F_{st} for a pair of cohorts¹. As each 1KG
864 reference population has a sample size around 100, there is no disproportionate impact of
865 sample size in calculating F_{st} .

866

867 **F_{st} Cartographer algorithm.** The purpose of using the F_{st} Cartographer algorithm is to find
868 the coordinates of a cohort given its F_{st} to the reference populations. The algorithm can be
869 expressed in Cartesian geometry. Given three reference populations, a target cohort has three
870 F_{st} measures, F_1 , F_2 , and F_3 , respectively. Given a Cartesian coordinate system, the
871 coordinate for these three reference populations are (a_1, b_1) , (a_2, b_2) , and (a_3, b_3) ,
872 respectively. The algorithm tries to find the coordinates $(x, y)_{E_{i,j}}$ on each the edge $(E_{i,j})$ that
873 connects reference populations i and j

$$874 \quad (x, y)_{E_{i,j}} = \left[(a_j - a_i) \frac{F_i}{F_i + F_j} + a_i, (b_j - b_i) \frac{F_i}{F_i + F_j} + b_i \right] \quad \text{(Equation 4)}$$

875 The coordinates of the gravity of triangle, $(x, y)_G$, that connects $E_{1,2}$, $E_{1,3}$, and $E_{2,3}$ are

$$876 \quad (x, y)_G = \left(\frac{x_{E_{1,2}} + x_{E_{1,3}} + x_{E_{2,3}}}{3}, \frac{y_{E_{1,2}} + y_{E_{1,3}} + y_{E_{2,3}}}{3} \right) \quad \text{(Equation 5)}$$

877

878 **Inference of cohort origins at the global level.** To assess genetic background, for each
879 cohort we calculated its F_{st} values using CEU, CHB, and YRI as the reference panel,
880 respectively. We denote these three F_{st} values as F_{CEU} , F_{CHB} , and F_{YRI} . These values reflect

881 genetic distances between a cohort and the reference panels - the greater the value the further
882 the genetic distance. We developed an algorithm called F_{st} cartographer, which can map a
883 cohort to global genetic variation as previously observed using individual level data from
884 principal component analysis⁶. The steps in the algorithm are as follows (**Supplementary**
885 **Fig. 1**):

886

887 Create the coordinates for the reference samples. Without loss of generality, these three
888 reference populations form an equilateral triangle, and we set the length of each edge to
889 unity. For example, the coordinates CEU, CHB, and YRI are $(-\sqrt{3}, 1)$, $(\sqrt{3}, 1)$, and $(0, -2)$,
890 respectively, and connecting the coordinates of the three reference populations formed an
891 equilateral triangle - the reference space. The gravity of this equilateral triangle is the
892 origin of the Cartesian space. The choice for the coordinates for the reference population is
893 arbitrary.

894

895 **Step 1 Create a cohort triangle using Equation 4.** Finding a point the distances of that to
896 both ends, which represent two populations, is proportional to the ratio of the F_{st} values of
897 the cohort to these two reference populations. Similarly, find the points on the other two
898 edges. For example, Finland Twin Cohort (FTC) had $F_{CEU} = 0.0102$, $F_{YRI} = 0.153$, and
899 $F_{CHB} = 0.099$. On the CEU-YRI edge, a point split the length to 0.0102:0.153, was
900 $(-1.72, 0.98)_{E_{1,2}}$; On the CEU-CHB edge into 0.0102:0.099, was $(-1.70, 1)_{E_{1,3}}$; and on the
901 YRI-CHB edge into 0.153:0.099, was $(1.05, -0.18)_{E_{2,3}}$. Connecting the three coordinates
902 created a “FTC” triangle inside the reference triangle.

903

904 **Step 2 Find the gravity of the cohort triangle using Equation 5.** The gravity of the “FTC”
905 triangle had its coordinates of $(-0.79, 0.60)_{G_{FTC}}$, which is inferred as the geographic
906 coordinates for FTC in F_{PC} space. It had relative distances of 1.03, 2.55, and 2.72 to CEU,
907 CHB, and YRI, respectively. The shorter the distance, the closer the genetic background is.

908

909 **Step 3 Repeat Steps 1, and 2 until the gravity of each cohort is found.**

910

911 Plots of the coordinates for each cohort will show the relative distance of each cohort to the
912 reference samples. If a cohort has equal distances to three reference populations, its gravity
913 will be close to the origin of the reference triangle.

914

915

916 **Method II: Principal component analysis for cohort-level allele**
917 **frequencies**

918 PCA has been widely used in genetics⁷ and recently proposed for controlling population
919 stratification for GWAS^{8,9}. We provide a new method that uses cohort-level allele
920 frequencies, often provided as summary statistics in meta-analysis. We call the new method
921 as meta-PCA.

922
923 Meta-PCA is based on a $G = (C + K) \times M$ matrix, which includes K reference populations
924 and C cohorts of question on M markers. In G , the m^{th} column represents the reported
925 reference allele frequencies for the m^{th} marker for $(K+C)$ cohorts. The kernel correlation
926 matrix for PCA is constructed on $\Sigma = G_s \times G_s^T$, in which G_s is the standardization for G for
927 each locus (on each column of G). Compared with individual-level data PCA, in the context
928 of meta-PCA each cohort can be viewed as an individual in the conventional sense. Given Σ
929 matrix, all the implementation is the same as the individual-data PCA.

930

931 There are efforts in establishing genetic interpretation for PCA^{8,10-12}. The interpretation of
932 meta-PCA could be approached by F_{pc} as described in the last section.

933

934 **Method III: The detection of overlapping samples with λ_{meta}**
935 **Inference of cohort origins at the within-Europe level.** To assess genetic background, for
936 each cohort we calculated its F_{st} values using CEU, FIN, and TSI as the reference panel, with
937 coordinates $(-\sqrt{3}, 1)$, $(\sqrt{3}, 1)$, and $(0, -2)$, respectively. For FTC, it had F_{st} values of 0.0102,
938 0.0052, and 0.0157, to CEU, FIN, and TSI, respectively. Using the F_{st} Cartographer
939 algorithm, the gravity of the FTC triangle had its coordinates of $(0.274, 0.361)_{G_{FTC}}$. It had
940 relative distances of 2.10, 1.59, and 2.42, to CEU, FIN, and TSI, respectively.

941
942 **Genealogical subspace.** Furthermore, we partition the F_{PC} space into three subspaces. For
943 example, given coordinates of $(-\sqrt{3}, 1)$, $(\sqrt{3}, 1)$, and $(0, -2)$, for CEU, FIN, and TSI,
944 respectively, connecting the origin and the coordinates for any two reference populations
945 created a subspace, which is defined as a genealogical subspace. We had three genealogical
946 subspaces: CEU-FIN genealogical subspace, CEU-TSI genealogical subspace, and FIN-TSI
947 genealogical subspace, respectively. If a cohort is located inside a subspace, it indicates that
948 this cohort may be derived from these two reference populations that creates the genealogical
949 subspace.

950
951 For European cohorts, the coordinates calculated from F_{st} Cartographer algorithm mirror the
952 origins of geographic locations of the cohorts, similar, but less refined, to what has been
953 observed in previous studies using individual level data for European samples^{13,14}.

954
955 **Effective number of overlapping samples (n_o).** If a pair of cohorts has overlapping
956 samples, it leads to a correlation of the estimated genetic effects for each locus. In the recent
957 literature, two kinds of correlation due to overlapping samples were introduced. The first one
958 was defined by directly calculating correlation between all estimated test statistics, $r =$
959 $cor(Z_1, Z_2)$, in which Z is a vector of M matched loci between two cohorts^{15,16}. The second
960 one was defined on the correlation for single locus given overlapping samples, as introduced
961 by Lin and Sullivan¹⁷. We used the second definition, and then extended the correlation due
962 to any relatives, a generalization of Lin and Sullivan.

963
964 For a pair of cohorts of sample sizes n_1 and n_2 ($n_1 \geq n_2$), for M matched loci which have
965 GWAS summary statistics, for example additive effects and their standard errors. For the m^{th}
966 locus, estimated association effect sizes are $b_{1,m}$ and $b_{2,m}$ with sampling variance $\sigma_{b_{1,m}}^2$ and
967 $\sigma_{b_{2,m}}^2$, respectively. b_1 is assumed to be drawn from a normal distribution $N(b_{1,m}, \sigma_{b_{1,m}}^2)$, and

968 $b_2 \sim N(b_{2,m}, \sigma_{b_{2,m}}^2)$. In cohort 1, $w_{1|k} = \frac{n_{12|k}}{n_1}$ is proportion of samples with a k^{th} -degree
 969 relatives in cohort 2 with $n_{12|k}$ the number of relatives of k th degree relatives shared between
 970 the samples; the phenotypic variance is assumed to be the same across the cohorts for a
 971 quantitative trait. For a locus, the genetic effect is estimated by linear regression $y_1 = a +$
 972 $b_1x + e$ in cohort 1 (the index for the locus is dropped for convenience). If the sampling
 973 variance of a locus is assumed to be the same for any subset of samples

$$b_1 = \frac{\sum_{k=0}^K w_{1|k} [E(y_{1|k}x_k) - E(y_{1|k})E(x_k)]}{\text{var}(x_m)} = \sum_{k=0}^K w_{1|k} b_{1|k}$$

974 The standard error of b_m is $\sigma_{b_1} = \sqrt{\frac{(1-h_{b_1}^2)\sigma_{y_1}^2}{n_1}} \approx \sqrt{\frac{\sigma_{y_1}^2}{n_1}}$, in which $h_{b_1}^2$ is the proportion of
 975 phenotypic variance explained by the locus and $\sigma_{y_1}^2$ is the phenotypic variance of the trait.

976 The sampling variance for $\sigma_{b_{1,k}} = \sqrt{\frac{\sigma_{y_1}^2}{w_{1|k}n_1}}$. This decomposition of the genetic effect can be
 977 applied to cohort 2. Consequently, the covariance between b_1 and b_2 for the locus is

$$\text{cov}(b_1, b_2) = \text{cov}\left(\sum_{k=0}^K w_{1|k} b_{1,k}, \sum_{k=0}^K w_{2|k} b_{2,k}\right) = \sum_{k=0}^K w_{1|k} w_{2|k} \text{cov}(b_{1|k}, b_{2|k})$$

978 in which $\text{cov}(b_{1|k}, b_{2|k}) = \rho_k \theta_k \sigma_{b_{1|k}} \sigma_{b_{2|k}}$ is the covariance between the genetic effects
 979 estimated in two cohorts due to the k -degree relatives. ρ_k is the phenotypic correlation for the
 980 k -degree relatives, and θ_k is the genetic relatedness for the k -degree relatives. $\theta_k = \left(\frac{1}{2}\right)^k$ is
 981 the coefficient of identity for descent. For duplicated samples, $\rho_0 = h^2 + \rho_{e|0}$, in which h^2 is
 982 the heritability, and $\rho_{e|0}$, the environmental correlation to be close 1 for overlapping samples;
 983 for other relatives ($k \geq 1$), $\rho_k \approx \theta_k h^2$.

984

985 **Correlation between the estimated genetic effects.** The covariance can be generalized as

986 $\text{cov}(b_1, b_2) = \sum_{k=0}^K \sqrt{w_{1|k} w_{2|k}} \rho_k \theta_k \sqrt{\frac{\sigma_{y_1}^2 \sigma_{y_2}^2}{n_1 n_2}}$. After adjustment by the sampling variance, the
 987 correlation between b_1 and b_2 is

$$988 \rho_{b_1, b_2} = \frac{\text{cov}(b_1, b_2)}{\sigma_{b_1} \sigma_{b_2}} = \frac{\sum_{k=0}^K \rho_k \theta_k \sqrt{w_{1|k} w_{2|k}}}{\sqrt{n_1 n_2}} = \frac{\sum_{k=0}^K \rho_k \theta_k n_{12|k}}{\sqrt{n_1 n_2}} = \frac{n_o}{\sqrt{n_1 n_2}} \text{ (Equation 6)}$$

989 in which $n_o = \sum_{k=0}^K \rho_k \theta_k n_{12|k}$, is the effective number of overlapping samples averaged over
 990 all relative pairs that are across the two cohorts. As the variance explained by each locus is
 991 small, and after further weighted by θ_k , the contribution from overlapping relative is small.
 992 When ignoring the first and higher degree relatives n_o equals the contribution from
 993 overlapping samples. This is consistent with the results from Lin and Sullivan¹⁷, who

994 considered overlapping samples only. So, the correlation at any single locus is largely
 995 determined by the overlapping samples ($n_{12|0}$) for summary statistics.

$$996 \quad \rho_{b_1, b_2} = \frac{n_o}{\sqrt{n_1 n_2}} \approx \frac{n_{12|0}}{\sqrt{n_1 n_2}} \quad \text{(Equation 7)}$$

997 So, in the text hereafter, n_e indicates overlapping samples only, otherwise specified.

998

999 **Correlation for case-control studies.** The theory above is based on a quantitative trait, but it
 1000 holds approximately true for case-control studies if a locus is from the null distribution of no
 1001 association with the disease. Given $n_{12.ctrl}$ overlapping controls and $n_{12.cs}$ overlapping cases,
 1002 for a locus associated with disease its correlation of the regression coefficient is $\rho_{b_1, b_2} =$

$$1003 \quad \frac{n_{12.ctrl} \sqrt{R_1 R_2} + n_{12.cs} \frac{1}{\sqrt{R_1 R_2}}}{\sqrt{n_1 n_2}}$$

as indicated by Lin and Sullivan¹⁷, in which R_i is the ratio between

1004 cases and controls in the i^{th} cohort. When it is balanced case-control design – $R = 1$,

$$1005 \quad \rho_{b_1, b_2} = \frac{n_{12.ctrl} + n_{12.cs}}{\sqrt{n_1 n_2}} = \frac{n_o}{\sqrt{n_1 n_2}}$$

resembles the correlation for quantitative traits. However, it

1006 should be noticed that for case control data, n_e is confounded with the number of overlapping
 1007 cases and controls.

1008

1009 **Theory for λ_{meta} .** For the summary statistics between a pair of cohorts for the m^{th} locus, we
 1010 can construct a statistic

$$1011 \quad T_m = \frac{(b_{1,m} - b_{2,m})^2}{\sigma_{b_{1,m}}^2 + \sigma_{b_{2,m}}^2} = \left[\frac{(b_{1,m} - b_{2,m})^2}{\sigma_{b_{1,m}}^2 + \sigma_{b_{2,m}}^2 - 2\rho_{1,2} \sigma_{b_{1,m}} \sigma_{b_{2,m}}} \right] \times \left[\frac{\sigma_{b_{1,m}}^2 + \sigma_{b_{2,m}}^2 - 2\rho_{1,2} \sigma_{b_{1,m}} \sigma_{b_{2,m}}}{\sigma_{b_{1,m}}^2 + \sigma_{b_{2,m}}^2} \right] \quad \text{(Equation 8)}$$

1012 in which $\rho_{1,2}$ is the correlation between $b_{1,m}$ and $b_{2,m}$.

$$1013 \quad E(T_m) = \left\{ \frac{\sigma_{b_{1,m}}^2 + \sigma_{b_{2,m}}^2 - 2\rho_{1,2} \sigma_{b_{1,m}} \sigma_{b_{2,m}}}{\sigma_{b_{1,m}}^2 + \sigma_{b_{2,m}}^2 - 2\rho_{1,2} \sigma_{b_{1,m}} \sigma_{b_{2,m}}} + \frac{[E(b_{1,m}) - E(b_{2,m})]^2}{\sigma_{b_{1,m}}^2 + \sigma_{b_{2,m}}^2 - 2\rho_{1,2} \sigma_{b_{1,m}} \sigma_{b_{2,m}}} \right\} \left\{ \frac{\sigma_{b_{1,m}}^2 + \sigma_{b_{2,m}}^2}{\sigma_{b_{1,m}}^2 + \sigma_{b_{2,m}}^2} - \right.$$

$$1014 \quad \left. \rho_{1,2} \frac{2\sigma_{b_{1,m}} \sigma_{b_{2,m}}}{\sigma_{b_{1,m}}^2 + \sigma_{b_{2,m}}^2} \right\} = (1+H)(1-\rho_{1,2}\kappa) \quad \text{(Equation 9)}$$

$$1015 \quad \text{in which } H = \frac{[E(b_{1,m}) - E(b_{2,m})]^2}{\sigma_{b_{1,m}}^2 + \sigma_{b_{2,m}}^2 - 2\rho_{1,2} \sigma_{b_{1,m}} \sigma_{b_{2,m}}}, \kappa = \frac{2\sigma_{b_{1,m}} \sigma_{b_{2,m}}}{\sigma_{b_{1,m}}^2 + \sigma_{b_{2,m}}^2} = \frac{2\sqrt{n_1 n_2}}{n_1 + n_2}, \text{ and } \rho_{1,2} = \frac{n_o}{\sqrt{n_1 n_2}}, \text{ as}$$

1016 defined in Equation 7, is the correlation for this locus due to overlapping samples between
 1017 this pair of cohorts. Of note, $\rho_{1,2}$ is same for each locus regardless of a null locus or a locus
 1018 associated to genetic effects. For convenience, the subscript b was dropped in the text
 1019 hereafter.

1020

1021 Under the null hypothesis of no heterogeneity ($H = 0$) and no correlation ($\rho_{1,2} = 0$), $T_0 \sim \chi_1^2$,

1022 a standard 1-degree-of-freedom chi-square distribution. $\rho_{1,2} = \frac{n_o}{\sqrt{n_1 n_2}}$, in which n_o is the

1023 effective number of overlapping samples. Of note, since the majority of markers are likely
1024 sampled from the null distribution or have very small effect sizes, we can approximate
1025 $E(b_{1,m}) = 0$ and $E(b_{2,m}) = 0$, and therefore $H \approx 0$ for most marker pairs between a pair of
1026 cohorts. For the m^{th} marker that is in linkage disequilibrium with causal variants, $E(b_{1,m}) =$
1027 $\sum_{j=1}^{J_1} \beta_{1,j} \ell_{1,j}$, in which J_1 is the number of causal variants in linkage disequilibrium with the
1028 m^{th} marker for cohort 1, $\beta_{1,j}$ is the j^{th} causal variants in linkage disequilibrium with the m^{th}
1029 marker, and $\ell_{1,j}$ is the LD correlation between the m^{th} marker and the j^{th} causal variant¹⁸.
1030 Similarly for $E(b_{2,m}) = \sum_{j=1}^{J_2} \beta_{2,j} \ell_{2,j}$. If the cohorts are from the same ethnicity, the
1031 difference in the LD correlation can be ignored, for example for samples from cohorts with
1032 European ancestry. So, under a polygenic model H is expected to be zero, or close to zero.
1033
1034 The T statistic is calculated for each matched SNP between a pair of cohorts. After ordering
1035 all T values, we evenly sample 30,000 independent markers from the order statistic of all T
1036 values. Each pair of cohorts may sample T values based on 30,000 markers different from
1037 another pair of cohorts.

1038
$$\lambda_{meta} = \frac{median(T)}{median(\chi_1^2)} = 1 - \frac{2n_o}{n_1+n_2} \text{ (Equation 10)}$$

1039 in which $median(\chi_1^2) = 0.4549$. Under the null hypothesis of no heterogeneity and
1040 overlapping samples ($n_o = 0$), plotting the ordered T against its corresponding quartiles
1041 from χ_1^2 , will be along the diagonal, leading to $\lambda_{meta} = 1$. Heterogeneity between two
1042 cohorts, equivalent to a “negative” number of overlapping samples, will drive $\lambda_{meta} > 1$, and
1043 overlapping samples will make $\lambda_{meta} < 1$. The distribution of λ_{meta} can be assessed via the
1044 beta distribution, and λ_{meta} follows asymptotically a normal distribution $N(1,0.0136)$ given
1045 30,000 independent markers.

1046

1047 **Factors that influence λ_{meta} .** A number of factors will influence the λ_{meta} . 1) Sample
1048 overlap, including close relatives across cohorts, reduces the value of λ_{meta} (**Supplementary**
1049 **Fig. 2**) Conservative modeling, such as inclusion of covariates in the association model that
1050 are genetically correlated with the phenotype or the ‘genomic control’ approach (adjusting
1051 the sampling variance with λ_{GC} , $z = \frac{b}{\sqrt{\lambda_{GC}\sigma}}$), will inflate the sampling variance, and deflate
1052 λ_{meta} . 3) Genetic heterogeneity, which can be caused by differences in genetic architecture
1053 or methodological difference, will inflate λ_{meta} . 4) As characterized by Equation 10, the

1054 lower bound (cohort 2 is completed included in cohort 1, given $n_1 > n_2 = n_o$) of λ_{meta} is
1055 $1 - \frac{2}{\frac{n_1}{n_2} + 1}$, upon the ratio of the samples sizes of the two cohorts.

1056

1057 **Estimating overlapping samples.** As shown in Equation 10, λ_{meta} is a linear function of n_o ,
1058 hence the statistical power to detect overlapping samples is equivalent to asking how λ_{meta}
1059 departs from the null distribution. Assuming $H = 0$, the overlapping samples can be
1060 estimated as $\hat{n}_o = (1 - \hat{\lambda}_{meta}) \frac{(n_1 + n_2)}{2}$, and $\sigma_{\hat{n}_o} = \frac{n_1 + n_2}{2} \times 0.0136 \approx 0.0068(n_1 + n_2)$ given
1061 30,000 independent markers. Hence, using summary statistics only the proportion of
1062 overlapping samples can be estimated for quantitative traits. Given the type I error rate of
1063 0.05 ($\alpha = 0.05$), the statistical power for detecting \tilde{n}_o overlapping samples between two
1064 cohorts is $p = \Phi^{-1}(T, \tilde{n}_o, \sigma_{\tilde{n}_o})$, in which Φ^{-1} represents the accumulation power function of
1065 a normal distribution with the mean of \tilde{n}_o and standard deviation of $\sigma_{\tilde{n}_o}$. The statistical power
1066 is determined by T , the threshold for significance, \tilde{n}_o , the real overlapping samples, and $\sigma_{\tilde{n}_o}$,
1067 the standard deviation of the null hypothesis that there is no overlapping samples. Without
1068 loss of generality, $T = 1.96\sigma_{\tilde{n}_o} \approx 0.13(n_1 + n_2)$ given $\alpha = 0.05$. The 95% confidence
1069 interval is $[-0.13(n_1 + n_2), 0.13(n_1 + n_2)]$. The statistical power is maximized when
1070 $n_1 = n_2$, i.e. when a pair of cohorts has the same sample size.

1071

1072 For case-control studies, as $\hat{n}_o = n_{12.ctrl} \sqrt{R_1 R_2} + n_{12.cs} \frac{1}{\sqrt{R_1 R_2}}$, the estimate cannot
1073 distinguish between overlapping cases and overlapping controls; when $R_1 = 1$ and $R_2 = 1$
1074 (balanced case-control design for both cohorts), $\hat{n}_o = n_{12.ctrl} + n_{12.cs}$, indicating the overall
1075 overlapping samples between two cohorts, summed across cases and controls. If we know
1076 that only controls (cases) were shared between two cohorts, then $\hat{n}_o = n_{12.ctrl} \sqrt{R_1 R_2}$
1077 ($\hat{n}_o = n_{12.cs} \frac{1}{\sqrt{R_1 R_2}}$), so then an estimate of n_o indicates the number of overlapping controls
1078 (cases). Therefore, quantifying overlapping samples for case-control studies is more difficult
1079 than that for quantitative traits.

1080

1081

1082 **Method IV: Pseudo profile score regression (PPSR)**

1083 **PPSR** resembles the previously proposed Gencrypt method¹⁹, but PPSR is more powerful in
 1084 detecting various degree of relatives and more robust to missing data and imputation errors.

1085 For each individual, the PPS can be generated as below

1086 $A_i = S \times G_i$ (**Equation 11**)

1087 in which A_i is the PPS for the i^{th} individual, S is a $K \times M$ score matrix, and G_i is vector for
 1088 the genotypes for the chosen M loci.

1089 In detail,

$$\begin{bmatrix} a_{i1} \\ a_{i2} \\ \vdots \\ a_{iK} \end{bmatrix} = \begin{bmatrix} s_{11} & s_{12} & \dots & s_{1M} \\ s_{21} & s_{22} & \dots & s_{2M} \\ \vdots & \vdots & \ddots & \vdots \\ s_{K1} & s_{K2} & \dots & s_{KM} \end{bmatrix} \begin{bmatrix} g_{i1} \\ g_{i2} \\ \vdots \\ g_{iM} \end{bmatrix}$$

1090

1091 in which a_{ik} is the k^{th} profile score for the i^{th} individual, s_{km} is the additive effect at the
 1092 m^{th} locus (m from 1 to M) for the k^{th} profile score, and g_{im} is the standardized genotype at
 1093 the k^{th} locus for the i^{th} individual. Each s , the pseudo genetic effect, follows a standard
 1094 normal distribution $N(0,1)$; each pseudo genetic effect is independent to another. For each
 1095 PPS, $var(a_i) = \sum_{m=1}^M var(g_{im}s_k) = \sum_{m=1}^M g_{im}^2 var(s_k) = M$, in which s_k is the k^{th} column
 1096 for the S matrix, and on average each locus explains $\frac{1}{M}$ of the variation. For an individual a
 1097 pair of PPS, say a_{i1} and a_{i2} , has $cov(a_{i1}, a_{i2}) = \sum_{m=1}^M g_{im}^2 cov(s_{1m}, s_{2m}) = 0$.

1098

1099 Each PPS can be seen as a trait with $h^2 = 1$ because it does not have any sampling variance.

1100 For a pair of individuals, individual i and individual j , when both A_i and A_j have been

1101 standardized, their covariance for the k^{th} PPS $cov(a_{i1}, a_{j1}) = \theta h^2$, in which θ is the

1102 relatedness scores in terms of identity by state²⁰. Depending on the relatedness between a pair

1103 of individuals, $\theta = 1$ for monozygous twins or to a duplicated sample, $\theta = 0.5$ for first-

1104 degree relatives such as parent and offspring or full sibs. In general, for r^{th} -degree of

1105 relatives, $E(\theta_r) = 0.5^r$.

1106

1107 The theory presented above provides a theoretical basis for detecting overlapping samples

1108 using PPS other than sharing individual level genotypes. Assuming that each individual has

1109 K independent PPS (A_i having K elements), for individual i and j , we can regress A_i on A_j ,

1110 $A_i = \mu + bA_j + e_{ij}$ (**Equation 12**)

1111 in which μ is the grand mean, b is the regression coefficient, and e_{ij} is the residual. $E(b) =$

1112 $\frac{cov(A_i, A_j)}{var(A_j)} = \theta_r$. $E(b) = 0$ if individual i is not correlated with individual j , $E(b) = 0.5$ for

1113 first-degree relatives, and $E(b) = 1$ if individual i and j are genetically same, say an

1114 overlapping sample or the homozygous twins. The sampling variance of b is $\sigma_b^2 =$

1115 $\frac{\sigma_{A_i}^2 - \sigma_{A_j}^2 \theta_r^2}{\sigma_{A_j}^2 K} = \frac{1 - \theta_r^2}{K}$. Under the null distribution for no related or overlapping samples,

1116 $b \sim N(0, \frac{1}{K})$. The residual e_{ij} accounts the discordant genotypes, including missing genotypes

1117 and genotyping or imputation errors. For current GWAS data, after quality control, the

1118 discordant rate is often smaller than 1%.

1119

1120 If now we have C cohorts for which the individual genotypes of which cannot be disclosed to

1121 the central analysis hub, overlap between cohorts can be identified if PPS are supplied. By

1122 regressing their PPS to each other the overlapping individuals could be detected if $b \approx \theta_r$.

1123 Assuming there are N_c samples in each cohort, a total of $N = \sum_{c_1=1}^C \sum_{c_2>c_1}^C N_{c_1} \times N_{c_2}$

1124 regressions need to be carried out as defined in Equation 12. If we want to control the

1125 experiment-wise type I error rate α under the null hypothesis and type II error rate β (with

1126 power = $1 - \beta$) for $b = \theta_r$, the required number of pseudo profile scores for each individual

1127 is

1128
$$K \geq \left(\frac{z_{(1-\beta)} \sqrt{1-b^2} + z_{(1-\alpha)}}{b} \right)^2 \quad \text{(Equation 13)}$$

1129 in which $z_{(1-\beta)}$ and $z_{(1-\alpha)}$ are z scores under the given p -values at the subscripts. To

1130 accommodate technical errors, such as missing genotypes and genotype error, a cutoff of 0.95

1131 for b is adopted for detection of overlapping samples, and 0.4~0.45 for detecting first-degree

1132 relative.

1133

1134 The standardization of genotypes can either use the allele frequency from each cohort, or

1135 from a reference sample. Throughout the study, we used the allele frequency calculated from

1136 WTCCC bipolar disorder cohort as the reference, and using it as an approximation to

1137 standardize genotypes for all cohorts in comparison.

1138

1139 **Workflow for PPSR.** Given the statistical method for detecting overlapping samples as

1140 described above, the whole workflow for detecting can be split into three steps

1141 **(Supplementary Fig. 9).**

1142
1143 **In step 1, the required type I and type II error rates are defined and from that the**
1144 **required number of pseudo profiles to be generated.** The GWAMA central analyst selects
1145 consensus SNP markers across cohorts, and determines additive effects matrix S that will be
1146 used to generate pseudo profile scores for each cohort. In order to avoid strand issues, the loci
1147 having palindromic loci (A/T alleles or G/C alleles) are excluded.

1148
1149 **In step 2, each cohort generates PPSR for each individual with the set of consensus**
1150 **markers and the marker weights received from the GWAMA coordinator.** After
1151 generate the PPS, they send them back to the coordinator. This will be a file that contains N
1152 rows and K columns with pseudo-profile scores.

1153
1154 **In step 3, the coordinator runs PPSR for each sample in a cohort on each PPS generated**
1155 **for another cohort.** The final product of running PPSR is to generate a $n_i \times n_j$ matrix for a
1156 pair of cohorts, which have n_i and n_j samples respectively. For each pair of individuals in
1157 comparison, we take the one from cohort i as the response variable and from cohort j as the
1158 predictor variable in PPSR. In principle, swapping the response variable and the predictor
1159 variable do not affect the performance of PPSR. Each entry, the regression coefficient of
1160 PPSR, in the $n_i \times n_j$ matrix represents genetic similarity for these pair of individuals in
1161 comparison. Once the regression coefficients are above the threshold, it indicates there are
1162 samples duplicated. The central analyst can then request each cohort that is implicated in
1163 containing samples that are also in other cohorts to drop those samples, without revealing
1164 where the duplication occurred.

1165
1166 **Privacy issues when using PPSR.** As the exchange of the PPS is within a meta-analysis
1167 facility, it is not as vulnerable as that of releasing the GWAS summary to the public domain
1168 as discussed in previous studies^{21–23}. However, as PPS are generated from genotypes, it is
1169 worth to consider whether the PPS will reveal individual genotype information, or can be
1170 decoded from PPS. As a demonstration for the principle-of-proof, we consider to reverse
1171 Equation 11 to estimate genotypes. We consider the case where the additive effect matrix in
1172 Equation 11 is known, otherwise it is nearly impossible to recover genotype information.
1173 Given the workflow of PPSR, the analysts who coordinate the meta-analysis know the
1174 additive effect matrix, S in Equation 11, and receive PPS from each cohort have the
1175 information to decode genotypes that are employed to generate PPS.

1176

1177 After reversing Equation 11, using the standard regression method, the genotype in each
1178 locus can be estimated as

$$1179 \quad A_i = \mu + g_{im} \times s_{.m} + e \quad \text{(Equation 14)}$$

1180 In detail,

$$\begin{bmatrix} a_{i1} \\ a_{i2} \\ \vdots \\ a_{iK} \end{bmatrix} = \mu + g_m \begin{bmatrix} s_{im} \\ s_{im} \\ \vdots \\ s_{im} \end{bmatrix} + e$$

1181 in which $s_{.m}$ is the m^{th} column in the additive effects matrix in Equation 11. Although

1182 $E(g_{im}) = g_{im}$, which is an unbiased estimate of the genotype, its sampling variance is

$$1183 \quad \sigma_{g_{im}} = \sqrt{\frac{\sum_{m=1}^M [1 - (1 - p_m)^2] \sigma_{s_{.m}}^2}{K}}. \text{ The sampling variance can be further written as } \sigma_{g_{im}} =$$

1184 $\sqrt{\frac{M}{K} E(\mathcal{P}_m)}$ because $\sigma_{s_{.m}}^2 = 1$ and $[1 - (1 - p_m)^2]$ is denoted as \mathcal{P}_m . The greater the ratio

1185 between $\frac{M}{K}$ and $E(\mathcal{P}_m)$, the larger the sampling variance, and consequently the lower

1186 probability to construct the real genotype.

1187

1188 Without loss of generality, the accuracy of the estimated \hat{g} , a continuous variable, and g , a

1189 discrete variable with values of 2, 1, and 0, can be measure using the squared correlation

1190 $(R^2)^{24}$,

$$1191 \quad R^2 = \frac{E[\sigma_g^2]}{E[\sigma_g^2] + \frac{M}{K} E[g^2]} \quad \text{(Equation 15)}$$

1192 in which $E(g^2)$ and $E(\sigma_g^2)$ are:

$$E(g^2) = \tilde{p}_{AA} x_{AA}^2 + \tilde{p}_{Aa} x_{Aa}^2 + \tilde{p}_{aa} x_{aa}^2$$

$$E(\sigma_g^2) = \tilde{p}_{AA} (x)(x_{AA} - 2p)^2 + \tilde{p}_{Aa} (x_{Aa} - 2p)^2 + \tilde{p}_{aa} (x_{aa} - 2p)^2$$

1193 $x_{AA} = 2$, $x_{Aa} = 1$, and $x_{aa} = 0$ if A is the reference allele, and \tilde{p}_{AA} , \tilde{p}_{Aa} , and \tilde{p}_{aa} are

1194 weighted frequency given the distribution of g . $f = \tilde{p}_{AA} + 0.5\tilde{p}_{Aa}$.

1195

1196 When the reference allele frequency follows a uniform distribution between (a_1, a_2) ,

1197 assuming that the loci follow Hardy-Weinberg proportions, $p_{AA} = p^2$, $p_{Aa} = 2pq$, and

1198 $p_{aa} = q^2$, in which p follows a uniform distribution between a_1 and a_2 and $q = 1 - p$.

$$p_{AA} = \int_{a_1}^{a_2} p^2 = \frac{1}{3} p^3 \Big|_{a_1}^{a_2} = \frac{1}{3} (a_2^3 - a_1^3)$$

$$p_{AA} = \int_{a_1}^{a_2} 2pq = \left(p^2 - \frac{2}{3}p^3\right) \Big|_{a_1}^{a_2} = (a_2^2 - a_1^2) - \frac{2}{3}(a_2^3 - a_1^3)$$

$$p_{aa} = \int_{1-a_2}^{1-a_1} q^2 = \frac{1}{3}q^3 \Big|_{1-a_2}^{1-a_1} = \frac{1}{3}[(1-a_1)^3 - (1-a_2)^3]$$

1199 and $\tilde{p}_{AA} = \frac{p_{AA}}{p_{AA}+p_{Aa}+p_{aa}}$, $\tilde{p}_{Aa} = \frac{p_{Aa}}{p_{AA}+p_{Aa}+p_{aa}}$, and $\tilde{p}_{aa} = \frac{p_{aa}}{p_{AA}+p_{Aa}+p_{aa}}$.

1200

1201 If the reference allele frequency follows a uniform distribution between (0, 0.5), $R^2 =$

1202 $\frac{\frac{5}{12}}{\frac{5}{12} + \frac{2M}{3K}} = \frac{5}{5 + 8\frac{M}{K}}$.

1203

1204 Given M loci with MAF of 0.5, the expected frequencies for AA , Aa , and aa are $\tilde{p}_{AA} = 0.25$,

1205 $\tilde{p}_{Aa} = 0.5$, $\tilde{p}_{aa} = 0.25$, and $f = 0.5$. $E(g^2) = 1.5$, and $E(\sigma_g^2) = 0.5$. Plugging them in to

1206 the Equation 13 leads to $R^2 = \frac{0.5}{0.5 + 1.5\frac{M}{K}} = \frac{1}{1 + 3\frac{M}{K}}$.

1207 Equation 13 can be rewritten as $R^2 = \frac{1}{1 + \varphi\frac{M}{K}}$, in which $\varphi = 3$ if MAF is 0.5, and $\varphi = 1.6$ if

1208 MAF is nearly from a uniform distribution. From Equation 13, it is easy to calculate the ratio

1209 between the number of markers and the number of PPS given a controlled R^2 ,

1210 $\frac{M}{K} \geq \frac{1-R^2}{\varphi R^2}$ **(Equation 16)**

1211

1212 For uniform distribution of MAF, if $R^2 \leq 0.1$ is set as the threshold, $\frac{M}{K} \geq 5.4$; if $R^2 \leq 0.05$,

1213 $\frac{M}{K} \geq 11.4$, and if $R^2 \leq 0.01$, $\frac{M}{K} \geq 59.4$. In general, the higher the ratio between M and K , the

1214 less information can be inferred. We suggest $\frac{M}{K} \geq 5 \sim 10$ may be sufficient.